Design Criteria for Headed Stud Groups in Shear:

Part 1 – Steel Capacity and Back Edge Effects

Neal S. Anderson, P.E., S.E.
Consultant
Wiss, Janney, Elstner Associates, Inc.
Northbrook, Illinois

Donald F. Meinheit, Ph.D., P.E., S.E.
Senior Consultant
Wiss, Janney, Elstner Associates, Inc.
Northbrook, Illinois

The Precast/Prestressed Concrete Institute sponsored a comprehensive research program to assess the shear capacity of headed stud group anchorages. This program was initiated in response to new provisions introduced into the 2002 ACI 318 Building Code. The proposed ACI provisions are based on extensive data dominated by post-installed anchor tests. Tests of headed stud anchorages, as used in precast construction, are not prevalent in the literature. The test program, conducted by Wiss, Janney, Elstner Associates, Inc. (WJE), examined headed stud connections loaded toward a free edge, a free edge near a corner, parallel to one free edge, parallel to two free edges, away from a free edge, and in-the-field of a member, such that edge distance was not a factor. The information reported herein addresses the steel capacity failure mode. Test data were obtained when the shear force was directed away from a free edge, in-the-field testing, and from other edge distance tests where steel failure governed the capacity.

Headed stud anchorages are used extensively in the concrete industry in both cast-in-place and precast construction. Welding studs to steel plates provides an easy and economical means of embedding and providing a ready to complete structural connection. Such a connection has substantial versatility by allowing large variations in construction dimensions.

Headed stud anchorages in precast concrete members can be found in column corbels, spandrel beams, dapped-end members, wall panels, tee beams, and other components. Commonly, studs in precast members are 3 to 8 in. (76 to 203 mm) long and form multi-stud group connections. The load capacities of these connections are generally affected by stud spacings, edge distances, and member depth or thickness.

In the past, the design of stud anchorages usually followed procedures set forth in the PCI Design Handbook[1] or the nuclear structures code, developed by ACI Committee 349.[2] Until now, stud anchorage design has not been codified within the widely accepted Building Code Requirements for Structural Concrete,[3] as prepared by ACI Committee 318. However, an approach for the design of anchorages to concrete has been approved as Appendix D[4] of the upcoming ACI 318-02 Building Code. The ACI 318 Appendix D method is based on the Concrete Capacity Design (CCD) model proposed by Fuchs, Eligenhausen, and Breen.[5]

The ACI design approach necessarily must consider all types of cast-in-place and post-installed anchors. The design procedure in ACI 318-02 Appendix D is calibrated using a database heavily dominated by post-installed anchors. Anchorages used in precast concrete construction fall into a relatively narrow range of those considered in ACI 318-02 Appendix D.

For headed stud anchorages, the ACI design approach shows significantly different capacity under certain conditions than the approach used in the current PCI design model. The concrete break-out capacity calculated with the proposed ACI approach is typically lower than that predicted by PCI design procedures, particularly when edge and spacing distance effects on stud groups are considered.

The differences in capacity prompted the PCI to undertake a research program with the ultimate objective of improving design criteria for headed stud anchorage groups, a connection type commonly used by the precast concrete industry. The research project included an experimental program to provide the background information for modifying the ACI or PCI design approaches or to justify and refine the PCI design approach as currently published in the PCI Design Handbook.

This paper represents Part 1 of four parts included in this research program. The work reported herein presents findings on two of the six primary variables evaluated in this shear capacity study. The variables in the shear testing program included conditions that loaded the headed stud groups:

1. Toward a free edge (de3).
2. Toward a free edge at a corner (de3 and de1 simultaneously).
3. Parallel to one free edge (de1).
4. Parallel to two free edges (de1 and de2 simultaneously)
5. Away from a free edge (de4).
6. In-the-field of the member such that edge distance was not a factor in the failure.

Schematic representations of the de1, de2, de3, and de4 edge distances are provided in Fig. 1.

Stud anchorage behavior when the connection is loaded away from a free edge and in-the-field is discussed herein. These two conditions cause the capacity to consistently be one of steel failure.

This paper provides background information for the steel capacity equations in ACI 318-02 Appendix D. The remaining components of this shear research program including the front edge effects, side edge effects, and combined front and side edge effects or corner influences will be reported in future issues of the PCI JOURNAL.

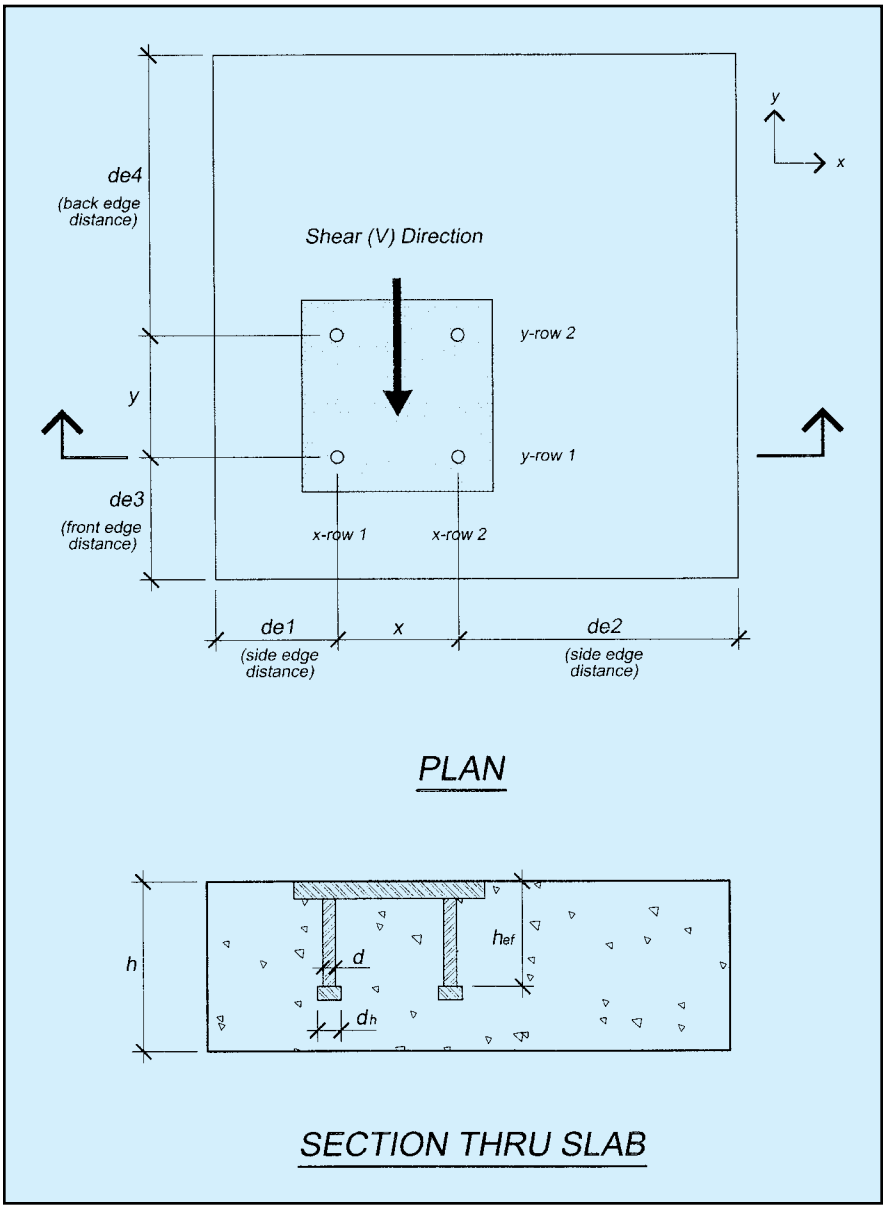

Fig. 1. Member geometry and edge distance notation after PCI definitions.

OVERVIEW OF RESEARCH PROGRAM

In mid-1996, PCI selected Wiss, Janney, Elstner Associates, Inc. (WJE) of Northbrook, Illinois, an engineering consulting firm, to undertake this research program under the direction

of PCI's Research and Development Committee. An advisory panel was appointed to closely monitor the project and consult on the testing scope. The advisory panel includes individuals from academia, consulting engineering, and precast concrete producer members.

Program Development

This research work[6] focused on anchorages and geometric conditions typically used in the precast/prestressed concrete industry. The research concentrated on diameter, embedment depth, and number of welded headed studs on a connection plate in configurations commonly used in precast concrete applications; the study excluded post-installed anchors.

The first task of the research program was to review existing data on headed studs embedded in structural concrete loaded in shear. Some experimental data on headed studs subjected to tension, shear, and combined tension and shear loadings have been published. However, the database for headed stud anchors is limited especially when compared to the database existing for post-installed anchors. Additionally, cast-in-place anchorages having head geometries similar to that of headed studs were included in this review, as applicable; for example, some cast-in-place anchor bolts fall in this category.

A literature search and analysis of existing data were used to formulate a laboratory test program. The shear testing program, conducted in the WJE laboratory, had the following objectives:

- Verify that a well-developed stud connection, that is, studs long enough to preclude a concrete pryout failure, located away from edge influences will develop a capacity dictated by characteristics of the stud steel properties.
- Evaluate group behavior near the side (de1), front (de3), and back (de4) free edges considering as variables: distance from an edge, spacing in the *x*- and *y*-directions, number of anchors in the group, embedment depth, and anchor diameter.
- Review or refine the concrete breakout model with respect to the de1, de3, and de4 edge distances.
- Determine the influence of the slab "thickness effect" for shear-loaded connections.
- Evaluate anchor group behavior at a corner, where the de1 and de3 edge distances meet.
- Evaluate anchor group behavior when simultaneous de1 and de2 edge conditions exist, such as in a column.

Table 1. Summary of the WJE/PCI test program.

Tests completed	328 shear tests performed
Test specimens	34 concrete slab specimens cast (12) 5 x 5 ft x 6 in. (4) 4 x 10 ft x 16 in. (3) 4 x 4 ft x 16 in. (15) 5 x 5 ft x 16 in. 16 push-off specimens utilizing a steel wide flange section
Fabrication	Six separate concrete castings made 40.5 cu yd of concrete used for an average of 6.5 cu yd per casting
Supporting tests	Concrete compressive and tensile strength Concrete modulus of elasticity Tensile strength of all headed stud sizes used (23 tests total) Double shear strength of all headed stud sizes used (18 tests total)
Stud sizes	$^1/_2$ ϕ x $3^1/_8$ in. $h_{ef} = 5.38d$ $^1/_2$ ϕ x $5^5/_{16}$ in. $h_{ef} = 9.84d$ $^5/_8$ ϕ x $4^3/_{16}$ in. $h_{ef} = 5.93d$
Anchorages	14 anchorage plate layouts 1, 2, 3, 4 and 6 stud combinations evaluated
Concrete strength	5000 to 6000 psi (typical of precast concrete)
Test locations	Front edge (de3) 102 tests Side edge (de1) 94 tests Back edge (de4) 23 tests Front corner (de1-de3) 67 tests In-the-field 26 tests Push-offs 16 tests

Note: 1 in. = 25.4 mm; 1 ft = 0.3048 m; 1 lb = 4.448 N; 1 kip = 4.448 N; 1 psi = 6.895 kPa; 1 ksi = 6.895 MPa; 1 cu yd = 0.7646 m^3.

Testing Program Description

The WJE experimental program included 312 plate configurations in shear and 16 push-off type specimens, as summarized in Table 1. The tests were typically conducted in slabs measuring 4 x 10 ft or 5 x 5 ft (1.2 x 3.0 m or 1.5 x 1.5 m) with either a 6 or 16 in. (152 and 406 mm) thickness. The 16 push-off specimen tests were conducted to simulate the shear loading conditions when an embedded anchor group is adjacent to two longitudinal edges simultaneously.

In the shear testing program, a total of 14 different plate designations were evaluated, which included different combinations of plate size, stud spacing, stud embedment depth, and stud diameter. A conscience decision was made that plate thickness and concrete compressive strength would not be variables in the test program. Headed stud diameters of $^1/_2$-and $^5/_8$-in. (12.7 and 15.9 mm) were tested in this program.

The test program evaluated the capacity of single and group connection configurations in several geometric conditions. Referring to Fig. 1, anchorages were tested toward the free edge (de3), at a corner, adjacent or parallel to a free edge (de1), and away from a free or back edge (de4). Addi-

tional testing was directed to evaluate connection capacity when it was positioned far away from the influence of an edge, or the so-called "in-the-field" tests. The in-the-field tests were anticipated to produce a better understanding of connection capacity when the stud steel governs the failure mode. Several test series were repeated in both 6 and 16 in. (150 and 400-mm) thick specimens to evaluate the effects of member thickness.

The test findings reported in this paper represent one part of an overall comprehensive report on the shear behavior of headed stud anchorages loaded in shear. Results reported here are limited to defining the capacity of the stud steel in shear.

LITERATURE REVIEW

The welded headed stud gained considerable research attention in the late 1950s and through the 1960s. The early research work on welded headed studs was focused on applications in the concrete slab-steel beam composite member. The headed stud was viewed to be an efficient and effective shear transfer device, replacing channels, angles, or fabricated spirals attached to the top flange of a steel beam. The headed stud arc welding process represented a labor and material cost savings over manual arc welding the aforementioned shapes to a steel beam.

Push-Off Tests

Testing to evaluate composite beam behavior typically utilized a push-off specimen to study shear transfer through the headed studs. The push-off test specimen commonly used a wide flange beam section sandwiched between two concrete slabs. Headed studs were welded to both flanges in some prescribed pattern or spacing and embedded into a thin concrete slab representing the composite deck slab. The concrete slab was usually reinforced to simulate a bridge deck. As shown in Fig. 2, the steel beam was held above both the top and bottom elevation of the slabs. Both the beam and two slabs were oriented vertically fitting conveniently into a universal testing machine.

Early composite beam research, using the push-off specimen, was conducted by Viest at the University of Illinois,[7] Slutter, Fisher and others at Lehigh University,[8,9] Baldwin, Dallum, and others at the University of Missouri-Columbia,[10,11,12] Goble at Case Western Reserve University,[13] Chinn at the University of Colorado,[14] and Hawkins at the University of Sydney.[15] These early test programs produced a significant amount of shear data on headed stud behavior with a particular emphasis on groups. Several of the push-off test failure loads were due to stud steel shear, which is relevant to this paper.

Review of the push-off test results provides good comparative data for headed studs loaded in pure shear. As stated earlier, previous testing on the headed stud connections used in precast concrete attachments is limited, especially when groups are considered. To evaluate group stud connections, with an emphasis on steel failure, there are no known published test results.

Most of the non-push-off testing programs were conducted by loading the connection toward a free edge with the intent of studying anchorages loaded in shear and failing in a concrete breakout mode. Therefore, published behavioral results on headed

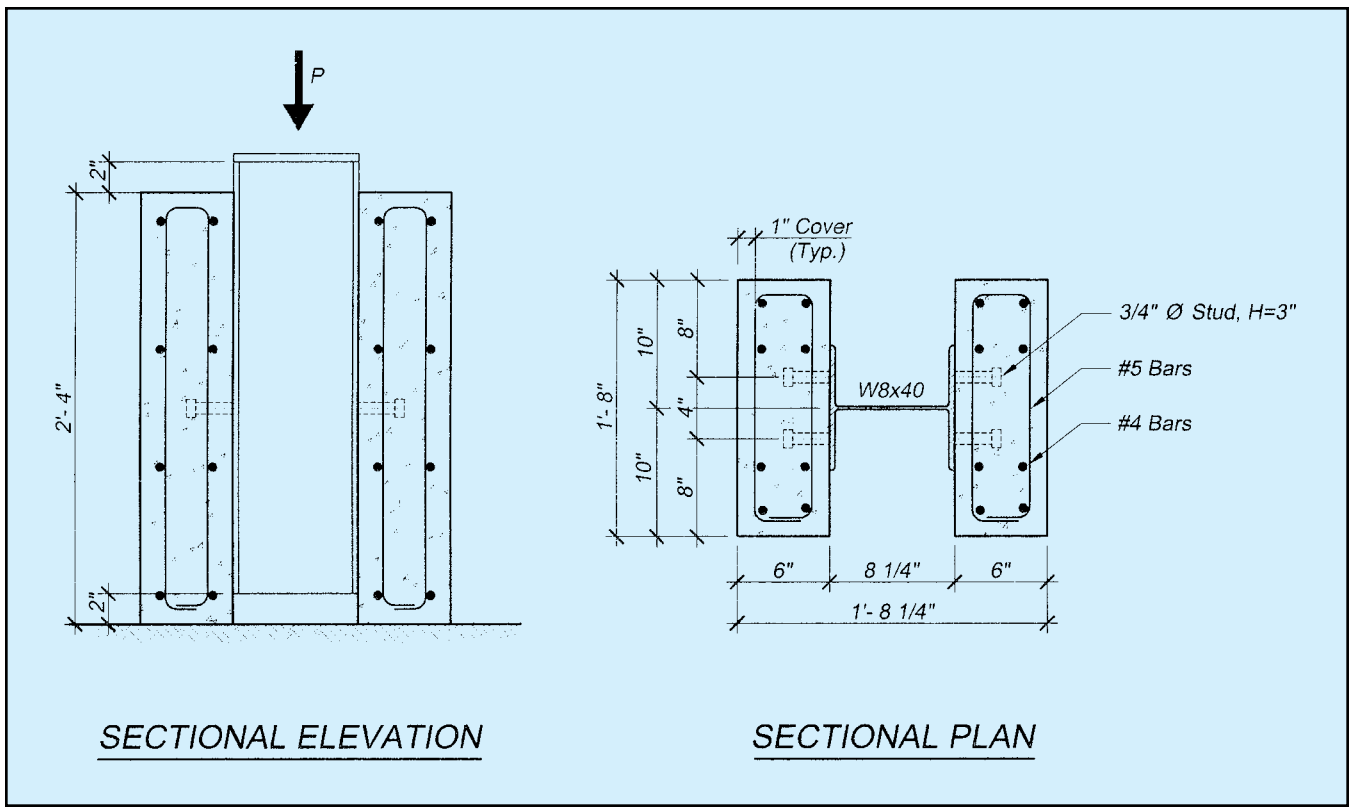

Fig. 2. Typical push-off test specimen (from Ollgaard, Slutter and Fisher).[9]

stud groups loaded in pure shear without the influence of any edge effects and failing the steel is entirely contained in the aforementioned referenced push-off tests.

It should be noted that the design of the push-off test specimen has characteristics that limit its full applicability to emulating a precast concrete anchorage. Most of the thin concrete slabs used in push-off tests contained nominal reinforcement, more representative of bridge deck construction. The reinforcement had no influence on the first cracking load, but it is likely-that the reinforcement in the concrete slab held the slab together to allow for additional displacement and ductility.

The early researchers were particularly concerned with load-slip characteristics of the connections. Unreinforced concrete specimens, reported in the literature, oftentimes produced a transverse splitting failure in the concrete slab, a failure mode unlikely to occur in actual bridge deck construction because of the presence of transverse reinforcement.

Another limitation of the push-off specimen relates to the mechanism to apply load to the embedded studs. Load transfer from the steel column through the headed studs into the two concrete slabs results in the best conditions to place the studs in pure shear. However, the external applied load causes a reaction against the ends of the two concrete slabs, placing them in compression. This condition is viewed to be analogous to a headed stud anchorage located in-the-field of a member; that is, a significant amount of concrete slab is located in front of the anchorage to preclude any front edge influences.

The favorable concrete compression stress developed in front of the studs does not affect tests having one transverse row (or one *y*-row) of studs. On the contrary, when stud groups with multiple longitudinal rows were tested using the push-off specimen, the test results become more difficult to interpret. Each longitudinal row in the group is subjected to a different level of compressive confinement stress. Likewise, multiple longitudinal (or *y*) rows which are spaced at large distances reduce the efficiency of the an-

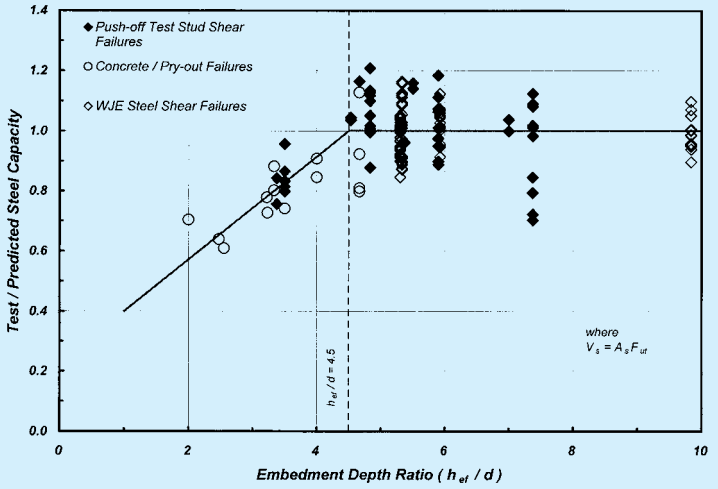

(a) Concrete and steel failures.

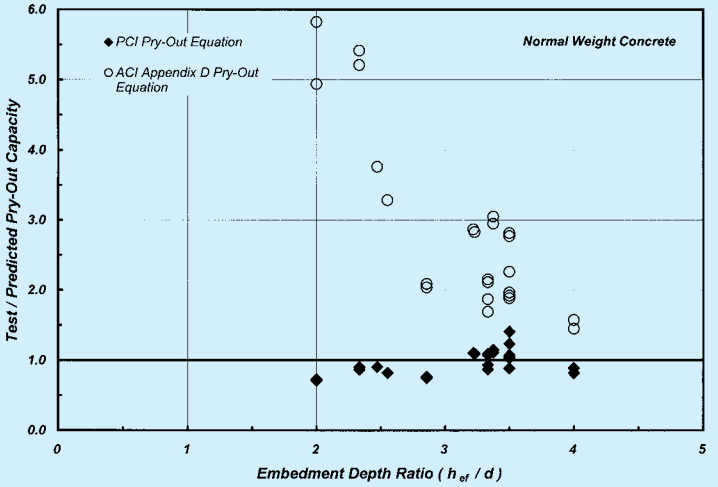

(b) Shallow embedment capacity predictions.

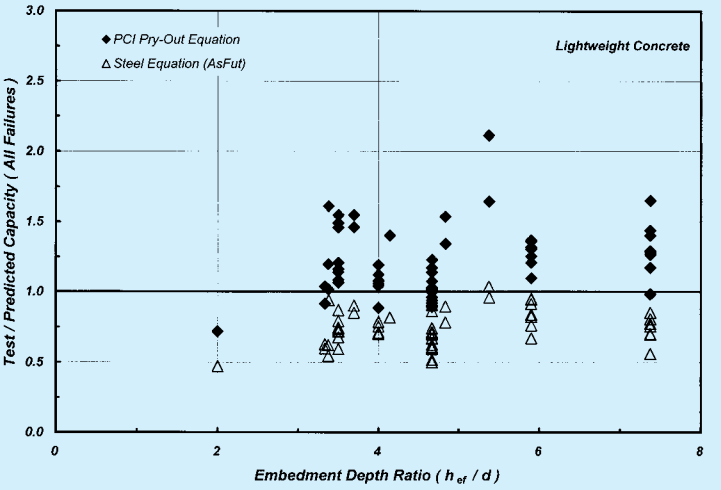

(c) Concrete and steel failures in push-off tests with lightweight concrete using PCI pryout capacity equation.

Fig. 3. Test-to-predicted capacity ratio as a function of embedment depth.

chor group due to shear lag effects.

A push-off specimen with multiple longitudinal rows of studs is similar to a long bolted connection whose efficiency is reduced in proportion to $\bar{x} / L$ (where $\bar{x}$ is the distance between the shear plane of the connected parts and the centroid of the connected component) in accordance with steel tension member design.

Our review of the available push-off data shows the overall connection length, L, may be a significant variable in determining the capacity that can be achieved by the stud because of shear lag. For further discussion of shear lag, see the book by Kulak, Fisher, and Struik.[16]

Keeping the above limitations of the push-off test in perspective, some valuable data were applicable to the present study. Relevant information from these early tests is discussed below.

Embedment Depth — In 1955, Viest[7] performed 12 push-off tests at the University of Illinois as part of research into composite beam behavior. Stud diameters ranged from 1/2 to 1 1/4 in. (12.7 to 31.8 mm), with a reasonably constant effective embedment depth (h_{ef}) between 3 and 3 1/2 in. (76.2 to 88.9 mm). All studs were placed in one row with an approximate 4 in. (101.6 mm) x-spacing for 10 of the 12 tests. Two tests had four, 3/4 in. (19.1 mm) diameter studs in one y-row with an approximate 2 in. (50.8 mm) center-to-center spacing. To ensure the studs were the only shear transfer mechanism, the steel I-beams were coated with grease to minimize any frictional transfer of the shear load along the flange width.

As reported in the work by Viest, the two-stud tests having ratios of effective depth to stud diameter (h_{ef}/d) of 4.53, 5.5, and 7.0 failed in stud shear (steel failure). The four tests with two studs having diameters of 1 and 1 1/4 in. (25.5 and 31.5 mm) experienced concrete failure. These four tests had average h_{ef}/d ratios of 3.22 and 2.51, respectively.

In the original Viest work, because the stud height was relatively constant, two prediction equations were presented for stud diameters less than 1 in. (25.4 mm) and greater than or equal to 1 in. (25.4 mm). In a subsequent research summary paper, Viest[17] described testing ten additional push-off specimens and modifying the equations for the 1957 AASHO Specifications. Instead of making the design equation a function of diameter only, the critical parameter became h_{ef}/d.

Another observation from the Viest test data is the apparent good correlation of steel shear capacity using a prediction of 1.0 $A_s F_{ut}$ when $h_{ef}/d \geq 4.53$. In this equation, A_s is the cross-sectional area of the stud shank and F_{ut} is the ultimate tensile strength of the stud steel.

This predicted steel shear failure load corresponds quite well to test data when-ultimate tensile strength of the steel is used, instead of a value reduced for tensile yield (F_y-= 0.9 F_{ut}), where F_y is the offset tensile yield stress for the stud steel. Likewise, it is a better predictor than the shear yield ($F_{vy} = 0.58 F_{ut}$, that is, $1/\sqrt{3}$), where F_{vy} is the shear yield stress according to the Huber-von Mises-Hencky yield criterion.[18]

WJE compiled push-off test data from a number of the referenced research studies to evaluate concrete and steel failures. To eliminate having the data influenced by shear lag, only push-off specimens with one longitudinal (y) row of studs were evaluated. Fig. 3(a) shows a graph of the test-to-predicted ratio for steel failure plotted against embedment depth ratio (h_{ef}/d), where the predicted capacity is based on 1.0 $A_s F_{ut}$.

The trend of the data indicates that 1.0 $A_s F_{ut}$ is a good predictor for a steel failure when the embedment depth (h_{ef}/d) exceeds about 4.5. This is just slightly greater than the value of 4.2 identified by Driscoll and Slutter[8] and incorporated into the 1961 AASHO Specifications.[19]

For some tests conducted in normal weight concrete, steel stud shear fail-

Table 2. Review of PCI Design Handbook requirements for stud strength governed by steel.

PCI Handbook edition	Parameters		Steel strength equation
	phi (ϕ)	Steel	
1 (1971)	none	f_s = 60 ksi	$V_u = 0.75\, A_{so} f_s$ $= 45.0\, A_{so}$
2 (1978) (shear-friction concept)	0.85	f_s = 60 ksi	$\phi V_c = \phi \mu A_b f_y$ $= 45.0\, A_b$ (where $\mu = 1.0$)
3 (1985)	1.0	f_s = 60 ksi	$\phi V_s = \phi\, (0.75)\, A_b f_s$ $= 45.0\, A_b$
4 (1992)	1.0	f_s = 60 ksi	$\phi V_s = \phi\, (0.75)\, f_s A_b n$ $= 45.0\, A_b n$
5 (1999)	0.90	f_y = 50 ksi	$\phi V_s = \phi\, (0.9)\, f_y A_b n$ $= 40.5\, A_b n$

Note: $A_{so} = A_b$ = cross-sectional area of the stud shank (sq in.); n = number of studs in the connection; f_s = ultimate tensile strength (ksi); f_y = yield strength (ksi).

Table 3. Minimum mechanical property requirements for headed studs adapted from AWS D1.1-2000.[31]

Property	Type A	Type B
Tensile strength (min.)	61,000 psi (420 MPa)	65,000 psi (450 MPa)
Yield strength (0.2 percent offset)	49,000 psi (340 MPa)	51,000 psi (350 MPa)
Elongation (min. percent 2 in.)	17 percent	20 percent
Reduction of area (min.)	50 percent	50 percent

ure occurred at embedment depth ratios (h_{ef}/d) less than 4.5. The tests with shorter stud embedment depths generally have predicted steel shear capacities (using 1.0 A_sF_{ut}) greater than the actual test results, even though the reported failure mode was that of stud failure. The steel failure mode may have, in fact, been a secondary failure after considerable concrete crushing or stud deformation had occurred.

Work performed by Ollgaard, Slutter, and Fisher[9] at Lehigh University was an extensive study using studs with an effective embedment depth (h_{ef}/d) of 3.26 and different types of lightweight and normal weight concrete. Failures were noted in both stud steel shear or by a concrete mechanism. Results of this work produced a prediction equation, independent of failure mode, basing individual stud strength on stud area, concrete compressive strength, and elastic modulus of the concrete. Their final prediction equation was:

$$Q_u = 0.5 A_s \sqrt{f'_c E_c} \qquad (1)$$

where

Q_u = nominal strength of a shear stud connector embedded in a solid concrete slab (kips)
A_s = effective cross-sectional area of a stud anchor (sq in.)
f'_c = specified compressive strength of concrete (ksi)
E_c = modulus of elasticity of concrete (ksi)

This equation is applicable to both normal and lightweight aggregate concrete. Unlike earlier prediction equations from the push-off test, this equation did not have a limitation on effective stud embedment depth, h_{ef}/d. This equation has a long history of being a good predictor of shear capacity, as it has been referenced in the AISC Specification since 1978.[20] In AISC, the upper bound on the stud strength is $A_{sc}F_u$, where A_{sc} is the cross-sectional area of a stud shear connector and F_u is the minimum specified tensile strength of the stud shear connector.

A simplified lower bound form of the Ollgaard, Slutter, and Fisher equation was proposed by Shaikh and Yi[21] in 1985:

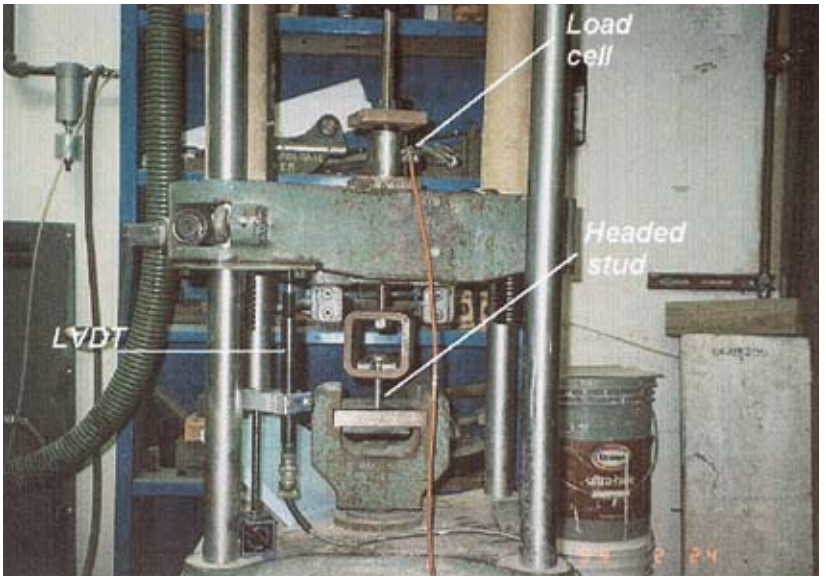

(a) Overall view of test setup.

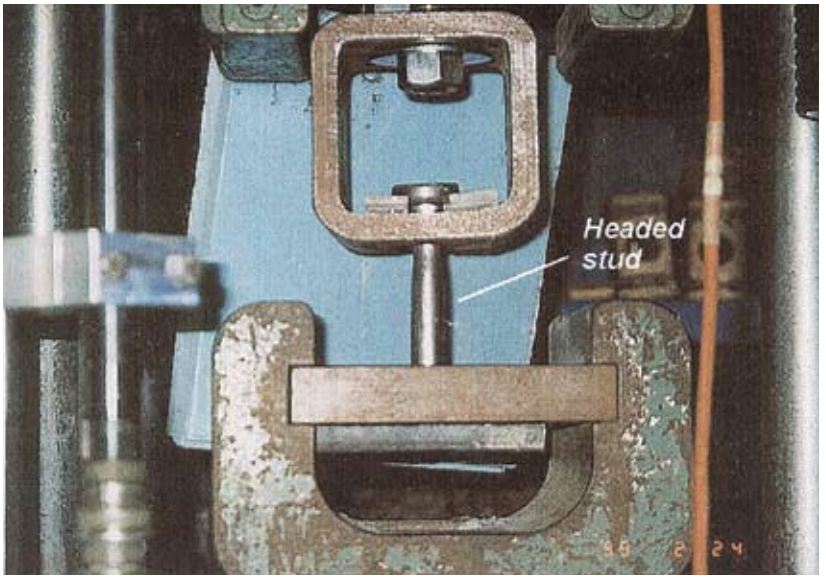

(b) Close-up view of test fixture.

Fig. 4. Test setup for tension testing headed studs welded to a steel plate.

$$V_{nc} = 800 \lambda A_s \sqrt{f'_c} \qquad (2)$$

where

V_{nc} = nominal shear strength (lb)
A_s = effective cross-sectional area of a stud anchor (sq in.)
f'_c = specified compressive strength of concrete (psi)
λ = concrete unit weight factor

The conversion of Eq. (1) to Eq. (2) with its assumptions and use of λ, resulted in an average prediction equation. Consequently, Shaikh and Yi selected a lower bound line through the data, resulting in a constant of 800. This equation appeared in both the Third and Fourth Editions of the PCI Design Handbook.

When the concrete failure test loads for short studs ($h_{ef}/d < 4.5$) in normal weight concrete are predicted in accordance with the PCI Design Handbook Fourth Edition[22] Eq. (6.5.8) [Eq. (2) above], there is reasonably good correlation with the data. The data plot in Fig. 3(b) shows the data trend with test-to-predicted capacities of about 1.0.

In summary, the work by Ollgaard, Slutter, and Fisher, as well as the WJE

review of other data showed that 1.0 A_sF_{ut} is a good predictor of steel stud shear capacity when $h_{ef}/d \geq 4.5$. When headed studs are shorter than this effective embedment depth, a concrete pryout failure mechanism occurs. Concrete pryout failure is a concrete breakout failure mode that is not a function of edge distance but a function of the "stiffness" of the headed stud. Thus for short, "stocky" anchors with h_{ef}/d less than 4.5 it appears that Eq. (6.5.8) in the Fourth Edition of the PCI Design Handbook, Eq. (2), appropriately predicts the concrete failure mode.

Lightweight Aggregate Concrete — Our analysis of reported steel shear failures in studs embedded in lightweight concrete indicates test strengths less than that predicted by 1.0 A_sF_{ut}. The data were found in the work by Ollgaard, Slutter, and Fisher;[9] Chinn;[14] and studies at the University of Missouri-Columbia.[11,12] Lightweight aggregate concrete appears to provide an embedment environment whereby the stud causes greater crushing of the concrete, producing more bending deformation, resulting in larger overall slip of the embedment.

On a macro level, lightweight concrete is a matrix of cement paste and lightweight aggregates. The cement paste, taken alone, has a higher compressive strength than the individual lightweight aggregate particles. In combination, this mixture usually does not exhibit a reduction in compressive strength over comparable normal weight concrete.

When a steel shear failure occurs, the welded end of the stud deforms by bending as it bears on the concrete. Extremely high, concentrated bearing stresses develop in the concrete, which eventually cause localized concrete crushing. Lightweight concrete has a lower concentrated point bearing strength than the point bearing strength in normal weight concrete because of the lightweight aggregate particles in the matrix. The weld connecting the stud to the plate concentrates the transfer of the shear load over a small bearing area in the concrete. As such, the bearing and localized crushing zone in the lightweight concrete needed for the concrete to mobilize bearing resistance is deeper.

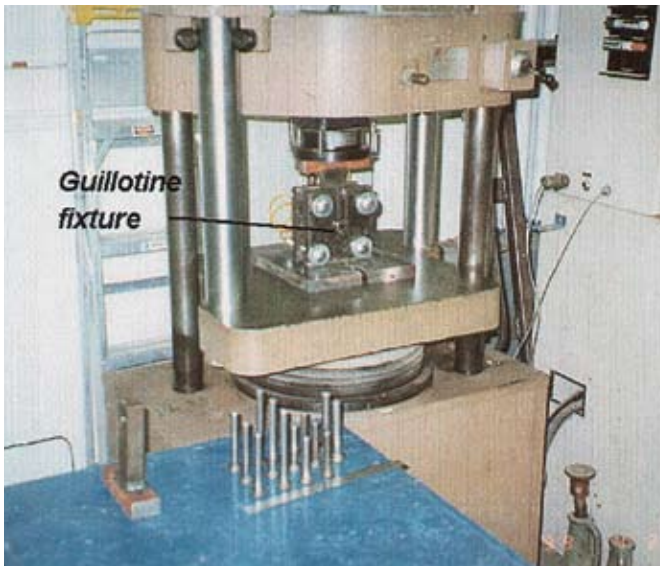

Fig. 5.
Test setup for shear testing of headed studs.

Lightweight concrete appears to allow the headed stud a greater opportunity to deform, and the increased concrete deformation induces more bending into the stud and attachment weld. The failure mode appears to be the result of combined shear and tension from the stud bending on the critically stressed portion of the weld.

In our analysis, this apparently higher bending deformation combined with shear deformation reduces the capacity of the headed stud to a lower value than 1.0 A_sF_{ut}. The stud shear capacity well away from a free edge in lightweight concrete is better predicted by Eqs. (1) or (2) for either concrete or steel failures, regardless of embedment depth, as shown in Fig.-3(c).

Connection Plate Thickness — To ensure adequate distribution of an applied shear force to the individual headed studs on a connection plate, the plate must have a certain minimum thickness. The PCI Handbook Fourth Edition[22] required the minimum plate thickness (t_{pl}) to be two-thirds the stud diameter ($t_{pl} \geq 0.67d$). The minimum plate thickness requirement was reduced in the Fifth Edition of the PCI Handbook[1] to one-half the stud diameter ($t_{pl} \geq 0.5d$).

Research on the minimum plate thickness appears to be limited to work by Goble at Case Western Reserve University.[13] This research focused on the minimum flange thickness required in light-gage steel in order to develop the full capacity of a welded stud connection. Goble determined the stud diameter-to-flange thickness (d/t_f) ratio was required to be less than or equal to 2.7 to develop the stud weld. A total of 41 push-off specimens were tested to develop this finding.

Alternatively written, the minimum flange thickness required must be greater than $0.37d$. Flange thickness meeting this minimum criterion exhibited steel stud shear failure. Thinner flanges, exceeding a d/t_f of 2.7, showed partial or full pullout of the stud from the flange, producing a divot or crater.

Based on this work, it appears that the current PCI minimum plate thickness requirements are slightly conservative when a connection is loaded in pure shear. An increased plate thickness may be justified when tension or combined shear and tension are considered to ensure more uniform load distribution to the stud group.

Minimum Slab Thickness — Steel stud failures, loaded in shear in the push-off specimens, were achieved in some relatively "thin" slabs. Review of the data shows steel failures occurred in slabs ranging in thickness from 4 to 7 in. (102 to 178 mm). For these tests, the clear cover over the head of the stud on the free surface side of the slab ranged from 1 to 3.1 in. (25.4 to 78.7 mm). A more convenient description is the slab thickness-to-effective embedment depth ratio (h/h_{ef}), which ranged from 1.4 to 2.2 for the published push-off test data.

No definite conclusions can be ex-

Table 4. Results of tensile tests on Nelson headed studs.

(1) Stud description	(2) Measured actual diameter (in.)	(3) Cross-sectional area (sq in.)	(4) Length before welding (BW) (in.)	(5) Length after welding (AW) (in.)	(6) Amount of burnoff (in.)	(7) Estimated stress at proport. limit (psi)	(8) Failure stress (psi)	(9) Diameter at fracture section (in.)	(10) Reduced cross-sectional area (sq in.)	(11) Percent reduction in area (percent)	(12) Percent elongation (percent)	(13) Failure in shank
1/2 in. x 3 1/8 in. (Heat F48266)												
WJE 1/12/99 (1)	0.494	0.1917	3.155	2.953	0.202	64174	81914	0.305	0.0731	61.9		X
WJE 1/12/99 (2)	0.494	0.1917	3.158	2.956	0.202	70435	82957	0.308	0.0745	61.1		X
WJE 1/12/99 (3)	0.494	0.1917	3.153	2.930	0.223	69392	82957	0.302	0.0716	62.6		X
Nelson 9/23/98	0.493	0.1909				64958*	82770			60.9	21.3	NR
Nelson 11/98	0.494	0.1917					77320					NR
WJE 1/15/99	0.494	0.1917				62609	81705	0.306	0.0735	61.6		X
Average	0.494			2.95		66653	81.60 ksi					
Std. dev.							2.17 ksi					
1/2 in. x 3 1/8 in. (Heat 792680)												
WJE 1/12/99 (4)	0.496	0.1932	3.145	2.963	0.182	66763	78667	0.293	0.0674	65.1		X
WJE 1/12/99 (5)	0.496	0.1932	3.152	2.926	0.226	64175	79184	0.291	0.0665	65.6		X
WJE 1/12/99 (6)	0.496	0.1932	3.154	2.991	0.163	69351	79184	0.286	0.0642	66.8		X
Nelson 4/14/98	0.494	0.1917				62609*	74348	0.316	0.0784	59.1	22.0	NR
WJE 1/5/99	0.496	0.1932				59518	76907	0.302	0.0716	62.9		X
Average	0.496			2.96		64952	77.66 ksi					
Std. dev.							2.07 ksi					
1/2 in. x 5/16 in. (Heat F48262)												
WJE 1/13/99 (7)	0.494	0.1917	5.335	5.205	0.130	56348	81392	0.312	0.0765	60.1		X
WJE 1/13/99 (8)	0.494	0.1917	5.343	5.212	0.131	53218	82957	0.303	0.0721	62.4		X
WJE 1/13/99 (9)	0.494	0.1917	5.346	5.201	0.145	55305	80870	0.315	0.0779	59.3		X
WJE 1/18/99 (D)	0.493	0.1909	5.347	5.199	0.148	58149	80675	0.312	0.0762	60.1		X
WJE 1/18/99 (E)	0.494	0.1913	5.346	5.188	0.158	54894	81034	0.305	0.0731	61.8		X
WJE 1/18/99 (F)	0.493	0.1909	5.346	5.187	0.160	58673	80151	0.320	0.0804	57.9		X
Nelson 9/23/98	0.493	0.1909				62863*	81198			61.4	21.0	NR
Average	0.494			5.20		56098	81.18 ksi					
Std. dev.							0.88 ksi					
1/2 in. x 5/16 in. (Heat F47841)												
WJE 1/18/99 (A)	0.493	0.1909	5.344	5.188	0.156	61554	81199	0.321	0.0809	57.6		X
WJE 1/18/99 (B)	0.493	0.1909	5.345	5.177	0.168	59982	79627	0.306	0.0733	61.6		X
WJE 1/18/99 (C)	0.493	0.1909	5.343	5.188	0.155	62863	80151	0.311	0.0760	60.2		X
Nelson 9/23/98	0.501	0.1971				60871*	75329	0.321	0.0809	58.9	21.0	NR
Average	0.495			5.18		61466	79.08 ksi					
Std. dev.							2.58 ksi					
5/8 in. x 4 3/16 in. (Heat A43765)												
WJE 1/13/99 (A)	0.624	0.3058	4.237	3.989	0.248	58205	76569	0.368	0.1064	65.2		X
WJE 1/13/99 (B)	0.623	0.3048	4.240	4.030	0.210	46582	72373	0.375	0.1104	63.8		X
WJE 1/13/99 (C)	0.624	0.3058	4.237	4.013	0.224	61475	76383	0.369	0.1069	65.0		X
WJE 1/18/99 (D)	0.623	0.3048	4.236	4.010	0.226	67577	83104	0.385	0.1164	61.8		X
WJE 1/18/99 (E)	0.623	0.3048	4.230	4.018	0.212	61673	81972	0.374	0.1099	64.0		X
WJE 1/18/99 (F)	0.624	0.3058	4.238	4.015	0.223	56897	81468	0.376	0.1110	63.7		X

*Column 7: 0.2 percent offset yield strength.
Column 13: NR denotes "Not Reported."
Note: 1 in. = 25.4 mm; 1 lb = 4.448 N; 1 psi = 6.895 kPa.

tracted from the push-off data regarding minimum slab thickness within the range tested. However, we conclude that slab thickness is not a variable influencing a stud steel shear failure.

***X*-Spacing Effect —** In early work by Viest,[7] a comparative set of tests was conducted with 3/4 in. (19 mm) diameter studs at differing *x*-spacings; that is, the distance between adjacent studs in one row. Tests 6A2 and 6B2 in that series had two studs in a transverse row with a 3.0 in. (99 mm) *x*-spacing. Companion specimens 6A4 and 6B4 had four studs across with a center-to-center spacing (*x*-spacing) of 1.9 in. (48.3 mm). All studs in these tests had embedment depth to stud diameter ratios (h_{ef}/d) greater than 4.5, such that the concrete pryout failure mode should not occur.

The two specimens with four studs in a row (Tests 6A4 and 6B4) failed in a concrete failure mode, even though their h_{ef}/d values were greater than 4.5. This implies that the anchor spacing in the *x*-direction can be a factor in the ultimate load capacity of the connection. In the ACI 318 Code Appendix D design provisions,[4] the minimum anchor spacing for multi-anchor connections is 4*d*. For the Viest tests with four studs in one row, the *x*-spacing ratio (x/d) was 2.5 while tests with two studs per row had a ratio of 4.0. Thus, it appears that if a minimum spacing of 4*d* is imposed on anchor spacing in a group with large edge distances, a steel failure should occur when h_{ef}/d is greater than 4.5.

Other than these tests by Viest, push-off tests by Goble[13] and Hawkins[15] studied conditions with h_{ef}/d greater than 4.5 and reported stud steel failure with a *x*-spacing as low as 4.8*d*. Other shear tests, exceeding a *x*-spacing of 4.8*d*, caused the stud to fail in shear.

PCI Design Handbook Review

Throughout the years, the PCI Design Handbooks[1,22-25] have contained upper limits on the strength of a headed stud connection loaded in shear. The maximum permissible shear load has always been limited by the stud's steel strength in shear. Table-2 summarizes the history of the PCI Design Handbook requirements for stud strength.

As shown in Table 2, the equations, strength reduction phi (ϕ) factors, and steel strengths (yield or ultimate tensile) used have varied. However, the basic resultant "allowable" stress on the stud has remained relatively constant at 45 ksi (310 MPa), assuming a minimum ultimate stud tensile strength (F_{ut} or F_s) of 60 ksi (414 MPa).

Aside from the information listed in Table 2, the Handbook has contained some unique provisions. The Second Edition incorporated the concept of shear-friction into the limiting equation. But the shear-friction coefficient, μ, was conservatively set equal to 1.0 based on the lack of test data.

The Third and Fourth Editions of the Handbook also contained a limitation on the concrete pryout strength equal to Eq. (2). As addressed earlier, this equation was a simplification to the Ollgaard, Slutter, and Fisher equation proposed by Shaikh and Yi. Eq. (2) was actually based on both concrete and steel failures. Note that Eq. (2) was dropped from the Fifth Edition of the Handbook.

Steel Code Review

The nominal shear strength of one stud connector embedded in a solid concrete slab is given in the AISC specifications[26] as Eq. (1). This pryout equation in AISC carries an upper limit of $A_{sc}F_u$. AISC does not specifically stipulate a separate phi reduction factor (ϕ) for studs. The reduction factor is apparently grouped with the bending phi factor, ϕ_b, which is 0.85 for plastic redistribution of stress or 0.90 for an elastic stress distribution on the section. These reduction factors are also calibrated to the AISC/ASCE load factors, which differ slightly from the traditional ACI load factors.

AISC does not place a limit on the effective stud embedment depth, h_{ef}/d. They do, however, place limitations on the stud spacing. The minimum center-to-center spacing of studs is to be 4*d* in the transverse direction, and 6*d* along the longitudinal axis of the composite beam. Finally, AISC limits the stud diameter to less than 2.5 times the flange thickness.

The code requirements in the Handbook of Steel Construction[27] from the Canadian Institute of Steel Construction (CISC)[27] are similar to AISC. The Canadian Code does place a capacity reduction factor (ϕ_{sc}) on the pryout equation, Eq. (1), while keeping the upper limit to $A_{sc}F_{ut}$. The phi resistance factor (ϕ_{sc}) is 0.80. Moreover, welded studs are to have an effective height to stud diameter ratio (h_{ef}/d) greater than 4.

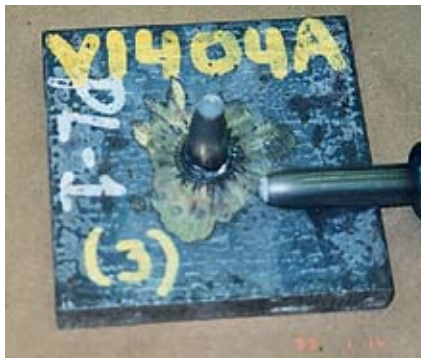

Fig. 6. Ductile failure of welded headed stud away from the weld.

Summary of Code Material Requirements

For the past 35 years, the material strength requirements for welded headed studs have remained unchanged. The 1965, Ninth Edition of the AASHO *Standard Specifications for Highway Bridges*,[28] representing the earliest codified properties, specified that shear connector studs should conform to ASTM A108 in Grades 1015, 1017, or 1020. The physical material properties listed in the 1965 AASHO were:

- Tensile strength (min.): 60,000 psi (415 MPa)
- Yield strength (min.): 50,000 psi (345 MPa) (0.2 percent offset)
- Elongation in 2 in. (52 mm) (min.): 20 percent
- Reduction of area (min.): 50 percent

These material properties are identical to the first requirements published by the American Welding Society (AWS) for shear connectors in the 1968 Supplement to AWS D1.0-66 and D2.0-66.[29] AWS also designated a second class of studs as "studs other than shear connectors" having the following material properties:

- Tensile strength (min.): 55,000 psi (380 MPa)
- Yield strength (min.): No requirement
- Elongation in 2 in. (52 mm) (min.): 20 percent

In the 1982 edition of AWS D1.1,[30] these lower strength studs were classed as Type A studs, whereas the 60 ksi (415 MPa) studs were classed as Type B studs.

The current *Structural Welding Code*, AWS D1.1 – 2000,[31] has recognized that mild steels conforming to ASTM A108[32] (Grades 1010 through 1020) and used for headed studs have increased material properties. Table 3, adapted from AWS D1.1-2000 Table 7.1, shows the current minimum tensile strength (F_{ut}) to be 65 ksi (450 MPa) and yield strength (F_y) to be 51 ksi (350 MPa) for Type B studs. Currently, AWS classifies Type B studs as studs that are headed, bent, or of other configuration in 1/2, 5/8, 3/4, 7/8, and 1 in. (12, 16, 20, 22, and 25 mm) diameters used as an essential component in composite beam design and other construction. The stud diameters listed appear to be the majority of those also used in precast concrete construction.

Type A studs cover the 1/4 and 3/8 in. (6 and 10 mm) diameter stud sizes, used occasionally in precast construction. As shown in Table 3, Type A studs currently have a 61 ksi (420 MPa) minimum tensile strength (F_{ut}) and a 49 ksi (340 MPa) minimum yield strength (F_y). AWS defines Type A studs as "general purpose of any type and size used for purposes other than shear transfer in composite beam design and construction."

STUD TESTS

Design rules for steel anchorages are generally based on the tensile properties of steel. For most design cases, it is convenient to base the capacity of headed studs on the tensile yield or strength values and relate the shear capacity to a factored reduction of either value. Materials used for manufacturing headed studs do not generally exhibit well defined yield point values. Therefore, the capacity of the stud is much easier to calculate when based on the easier to measure tensile strength. The headed stud properties

Table 5. Results of double shear tests on Nelson headed studs.

(1) Stud description	(2) Test number	(3) Measured actual diameter (in.)	(4) Cross-sectional area (sq in.)	(5) Length before welding (BW) (in.)	(6) Estimated stress at proportional limit (psi)	(7) Maximum shear stress (psi)	(8) Failure in shank	(9) Shear-Tensile data: Avg. shank tensile strength (psi)	(10) Shear-Tensile data: Ratio of shear to tensile strength
1/2 x 3 1/8 in. (Heat F48266) – Unrestrained									
WJE 4/21/99	1	0.494	0.1917	3.160	34174	49566	X		
WJE 4/21/99	2	0.493	0.1909	3.161	46624	56053	X		
WJE 4/21/99	3	0.493	0.1909	3.160	37718	51600	X		
Average		0.493	0.1911	3.160	39505	52406		81600	0.642
1/2 x 3 1/8 in. (Heat F48266) – Restrained									
WJE 4/23/99	1A	0.494	0.1917	3.159	34174	50870	X		
WJE 4/23/99	2A	0.494	0.1917	3.160	38087	55044	X		
WJE 4/23/99	3A	0.494	0.1917	3.164	45913	55305	X		
Average		0.494	0.1917	3.161	39392	53740		81600	0.659
1/2 x 3 1/8 in. (Heat 792680) – Unrestrained									
WJE 4/21/99	1	0.496	0.1932	3.151	32088	48132	X		
WJE 4/21/99	2	0.497	0.1940	3.148	36082	48196	X		
WJE 4/21/99	3	0.497	0.1940	3.148	35825	46392	X		
Average		0.497	0.1937	3.149	34665	47573		77660	0.613
1/2 x 5 5/16 in. (Heat F47841) – Unrestrained									
WJE 4/21/99	1	0.494	0.1917	5.347	34696	50609	X		
WJE 4/21/99	2	0.494	0.1917	5.345	34174	47479	X		
WJE 4/21/99	3	0.493	0.1909	5.345	35623	51338	X		
Average		0.494	0.1914	5.346	34831	49809		79080	0.630
1/2 x 5 5/16 in. (Heat F47841) – Restrained									
WJE 4/23/99	1A	0.494	0.1917	5.344	45653	54783	X		
WJE 4/21/99	2A	0.494	0.1917	5.345	46957	55826	X		
WJE 4/21/99	3A	0.494	0.1917	5.344	35218	55044	X		
Average		0.494	0.1917	5.344	42609	55218		79080	0.698
5/8 x 4 3/16 in. (Heat A43765) – Unrestrained									
WJE 4/21/99	1	0.624	0.3058	4.237	34171	51829	X		
WJE 4/21/99	2	0.625	0.3068	4.245	36669	51337	X		
WJE 4/21/99	3	0.624	0.3058	4.229	30411	50194	X		
Average		0.624	0.3061	4.237	33750	51120		78040	0.655

Note 1 : Tests identified with an "A" were run with side plates and the center plate, in the double shear test, having the same size drill holes. All other tests allowed the stud bearing on the side plates to rotate unrestrained.
Note 2: 1 in. = 25.4 mm; 1 lb = 4.448 N; 1 psi = 6.895 kPa.

used in these shear tests will also be related to the measured tensile strength properties of the stud.

Testing for Material Properties

Upon receipt of the headed stud materials from Nelson Stud Welding, WJE independently tested the geometry and physical characteristics for the various steel heats in the project stock. Four different stud length and diameter configurations were received. These headed studs were manufactured from six different heats of steel wire.

Headed studs were tested for their tensile and shear strength properties, in air. The test fixture was similar to that suggested in AWS D1.1-2000. Double shear, guillotine tests were also conducted on the middle third of the stud shank to determine the steel shear strength.

The steel plate for the test anchorages was purchased as ASTM A36 steel. Strength properties and chemical compositions of the plate steel were taken from mill test reports.

Test Setups

Direct Tension — A universal testing machine was adapted to test headed studs that had been welded to a square plate. The plate thickness was 1/2 in. (12.7 mm) in all cases. Both 1/2 and 5/8 in. (12.7 and 15.9 mm) diameter studs were evaluated. The photographs in Figs.-4(a) and 4(b) show the overall test setup and a close-up view for the welded, headed stud in the test fixture.

A load-deformation plot was made for each test. Deformation was measured between the cross-heads of the testing machine and, therefore, represents an overall behavior and not the actual stud shank strain.

Double Shear — Two different types of double shear, guillotine tests were conducted. The test setup, shown in Fig. 5, was essentially the same for both test types. A three-plate fixture was used similar to the typical push-off test specimen discussed earlier. The side plates contained either a slot or oversized hole. The interior plate reacted against the test machine head and was guided between the exterior plates, bearing on the stud. The fixture placed the studs in double shear.

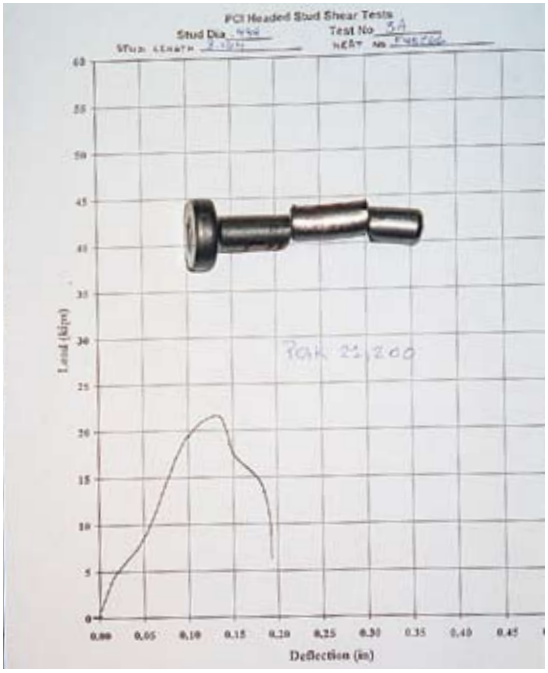

Fig. 7.
Shear failure of headed stud loaded in double shear.

The majority of tests allowed unrestrained rotation to occur in the stud shank as it was bearing against the two side plates. Some additional tests were conducted by drilling a hole slightly larger than the stud diameter through the side plate and thereby restraining the stud rotation.

Test Results

Tension — Tension test results and geometric properties for the various steel heats are listed in Table 4. Tests conducted in-house by Nelson Stud Welding are also incorporated into the table. The tensile test results typically accompanied the mill certificates for each steel heat.

Each tested stud exhibited a round-house load-deformation curve, requiring the 0.2-percent offset method to determine its yield strength. The stud yield strength was approximately 80 percent of the tensile strength.

All studs failed in a ductile manner forming a cup and cone fracture surface in the neck-down region, as shown in Fig. 6. The fracture was also consistently away from the weld. The reduction of area was approximately 60 percent for all tests.

Shear — Double shear test results are listed in Table 5. Two of the series were tested restrained and the remainder were unrestrained. The restrained tests, similar to the condition that may exist when the stud is embedded in concrete, had a slightly higher shear strength. The shear stress at the proportional limit is approximately 70 percent of the measured shear strength. A typical failure of the stud in double shear is shown in Fig. 7.

Plate Material Properties — Mill test reports showed that the flat bar stock used for the anchorage plates had an average yield stress of 47.6 ksi (328 MPa), an ultimate tensile strength of 70.1 ksi (483 MPa), and an elongation in 2 in. (51 mm) of 34.0 percent. Chemical analyses of the three steel heats used for the plates show an average carbon equivalent (CE) of 0.35 with a range of 0.33 to 0.37. The mechanical properties of the plate are on average less than those of the stud steel. The plate steel can be considered as very weldable for this test program.

Summary

Tables 4 and 5 summarize the measured tension and shear strength basic material properties. The tensile and yield strengths of each of these steel heats exceed the AWS D1.1-2000 requirements of 65 and 51 ksi (450 and 350 MPa), respectively. From these tension and shear tests, it would be expected that the shear strength of the headed stud embedded in concrete would be about 65 percent of the tensile strength, as shown in Table 5.

The average shear strength to tensile strength ratio for rivets, a similar fastening material to studs, has been reported to be about 0.75. This rivet shear to tensile strength ratio was seen to vary from 0.67 to 0.83 for the rivet tests. However, the data were independent of whether the rivet was driven or undriven, or on the grade of the rivet material.[16] The PCI Design Handbook reduces the design shear strength of headed studs by 10 percent presumably to account for the in-air shear strength to tension strength ratio being less than 1.0.

Earlier reported push-off test results indicate a shear strength behavior that is better than what these material test results imply.

SLAB TESTS

The majority of the shear tests in this test program were conducted with the anchors embedded in a concrete slab. A slab specimen is more representative of the conditions used in

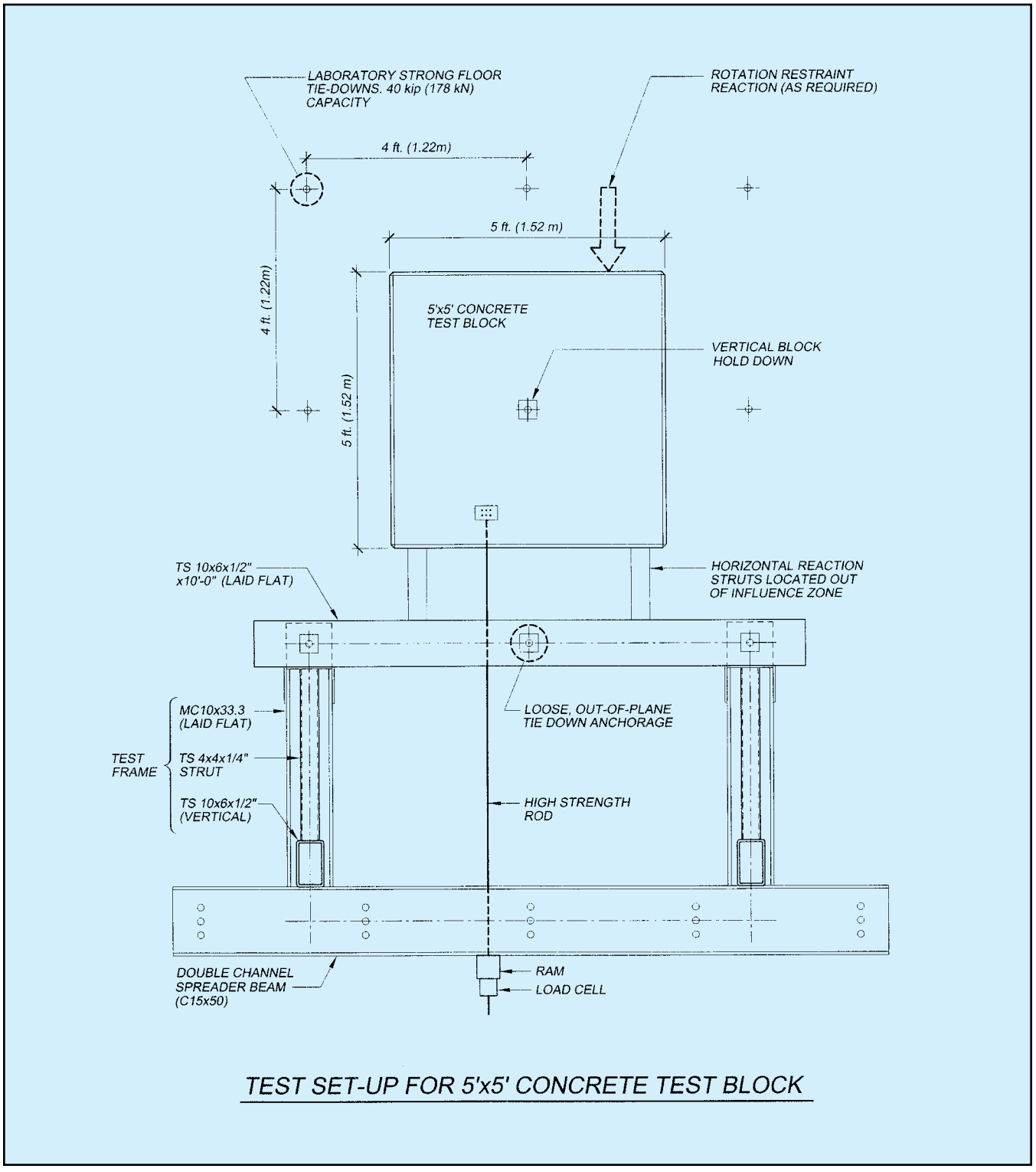

Fig. 8. Plan view of shear test setup.

precast construction than the push-off specimen.

Test Specimens

Two concrete slab sizes were selected for the investigation. The larger slab was a 4-x 10-ft (1.22 x 3.04 m) slab with a 16 in. (406 mm) thickness. Four of these slabs were fabricated because of their efficiency in locating edge shear tests. The large interior areas of these slabs were used for "in-the-field" tests, while the perimeter edges accommodated numerous test specimens with small edge distances. These large test slabs permitted many tests to be conducted without physically moving the specimen; only the loading apparatus needed to be repositioned.

Twenty-seven, 5 ft (1.52 m) square slabs were also fabricated in the test program. The slab thickness was either 6 or 16 in. (152 or 406 mm), constituting the variable range for the slab thickness effects. Because most in-the-field tests were contained in the larger slabs, this smaller square specimen proved efficient for laying out edge effect tests where spacing between the test samples needed to be large to avoid overlapping concrete breakout zones. The test anchorage locations were established to minimize the slab setup and handling during the tests.

Three additional 4 ft (1.22 m) square slabs, 16 in. (406 mm) thick, were cast during the course of the experimental work. These slabs were used to test conditions that were damaged by adjacent tests in earlier slabs or where repeated tests were needed.

All anchorage plates were 1/2 in. (12.7 mm) thick, Grade A36 (248 MPa) steel plate, having good weldability characteristics. Eight separate plate sizes, in plan, were used in the test program to accommodate the 14 different headed stud configurations.

Concrete selected for the test specimens was a commercially available 5000 psi (34.5-MPa), normal weight concrete mix containing 3/4 in. (19.1 mm) limestone coarse aggregate. All slabs were cast with the stud anchorage specimens in the bottom of the form to avoid conditions related to the so-called "top bar effect." This procedure was also used to ensure good concrete consolidation around the individual headed studs.

Reinforcement was only used in the 6 in. (152 mm) thick specimens for handling purposes. In these slabs, the reinforcement was placed so as not to interfere with the stud anchorage plates or provide confinement to the anchorage.

Testing

All slabs were tested flat (horizontal) on the laboratory test floor. Fig. 8 shows an overall plan view of the shear test specimen setup for a 5 ft (1.52 m) square slab test. Fig. 9 shows a cross-sectional view through the load application framework. Two triangular frames, of the shape shown in Fig. 9, were used to produce the shear force reaction. The frames were located 8 ft (2.45 m) apart and anchored to the laboratory strong floor.

A rectangular tube section, located between the test specimen and the triangular reaction frame, was used as a horizontal reaction beam for struts bearing against the bottom of the slab. A double channel spreader beam was elevated to the

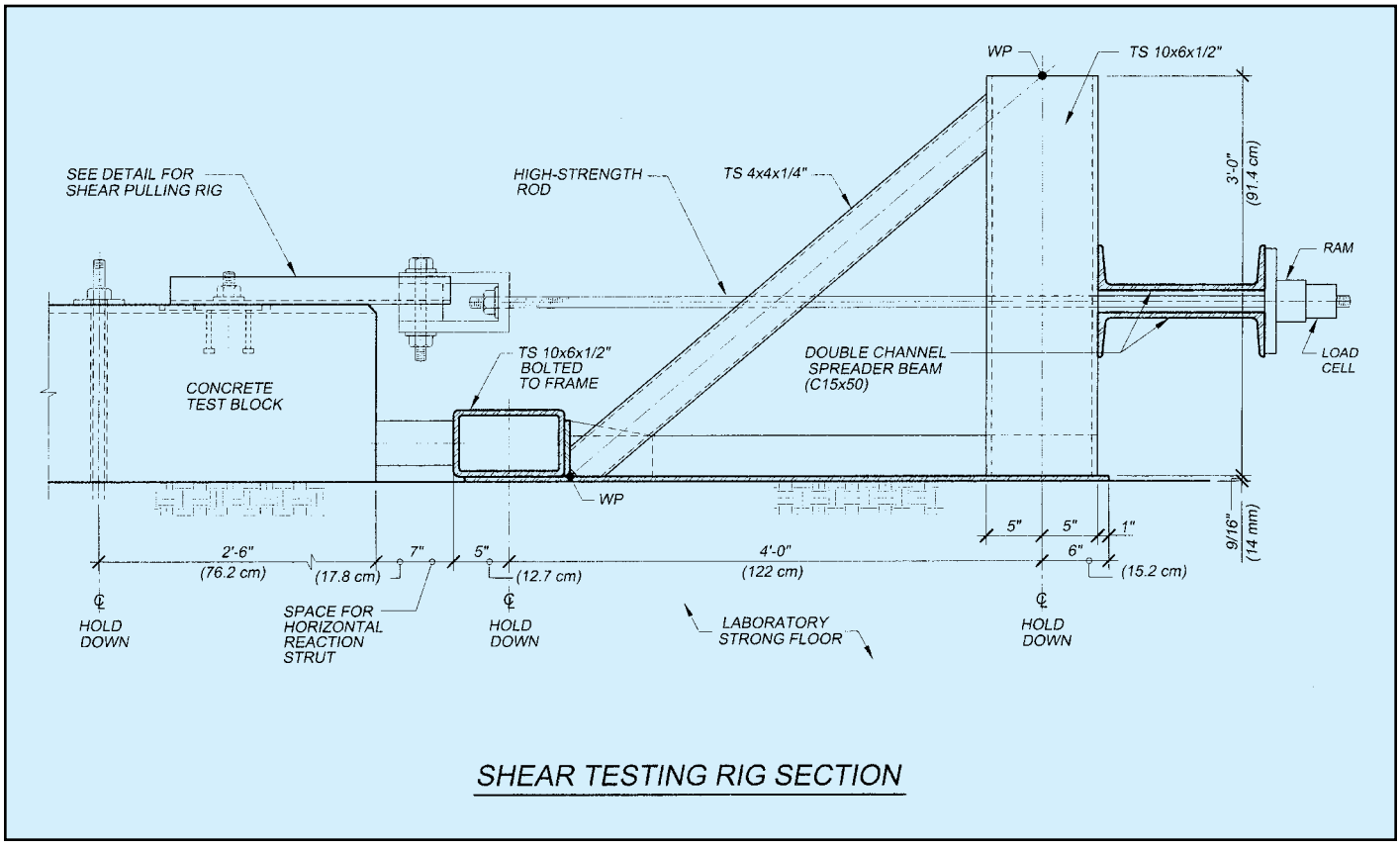

Fig. 9. Cross-sectional view of shear test setup.

proper height to react against the triangular test frame columns. A gap between the double channels accommodated a high strength, threaded rod, which was positioned through a center-hole ram and load cell.

At the concrete slab, the threaded loading rod was attached to a pinned clevis, which in turn was bolted to a channel shaped pulling device. As shown in Fig. 10, the channel shape had a shoe plate welded to the web (bottom), which reacted on the backside of the stud anchorage plate. This loading scheme was used in order to eliminate almost all eccentricity from the shear tests. Theoretically, the actual eccentricity was one-half the plate thickness or 1/4-in. (6.4-mm).

A threaded stud was used to "tie down" the channel and prevent it from "kicking up" while loading in the horizontal direction, as shown on Fig. 10. This threaded rod was stud welded to the exposed face of the plate prior to testing. During the test, the threaded stud was positioned in an oversized, slotted hole in the channel. To further ensure no shear resistance was provided at the threaded stud tie down, a teflon-coated plate washer was used below a finger-tightened nut.

All tests were instrumented with a load cell and two linear variable displacement transformers (LVDTs). The LVDTs measured the total movement of the plate parallel to the applied load. Digital data were collected through a data acquisition system linked to a personal computer. A peak-reading strain indicator, a voltmeter, and an analog *x-y* plotter were used to obtain real-time test data. Load was applied continuously with a center-hole hydraulic ram loading a 150 ksi (1034 MPa) threaded rod.

Following each test, the failure surface was documented with photographs and pertinent geometry was measured in the case of concrete breakout failures.

TESTS LOADING AWAY FROM A FREE EDGE (de4)

Shear load on anchorages directed away from a free edge is not commonly encountered in precast construction. However, special situations or framing conditions may dictate use of this type of connection. Pilot tests[33] conducted at the University of Wisconsin-Milwaukee (UWM), serving as a precursor for the present study, showed a potential concrete breakout/pryout failure mode associated with this edge condition connection. However, an eccentric shear

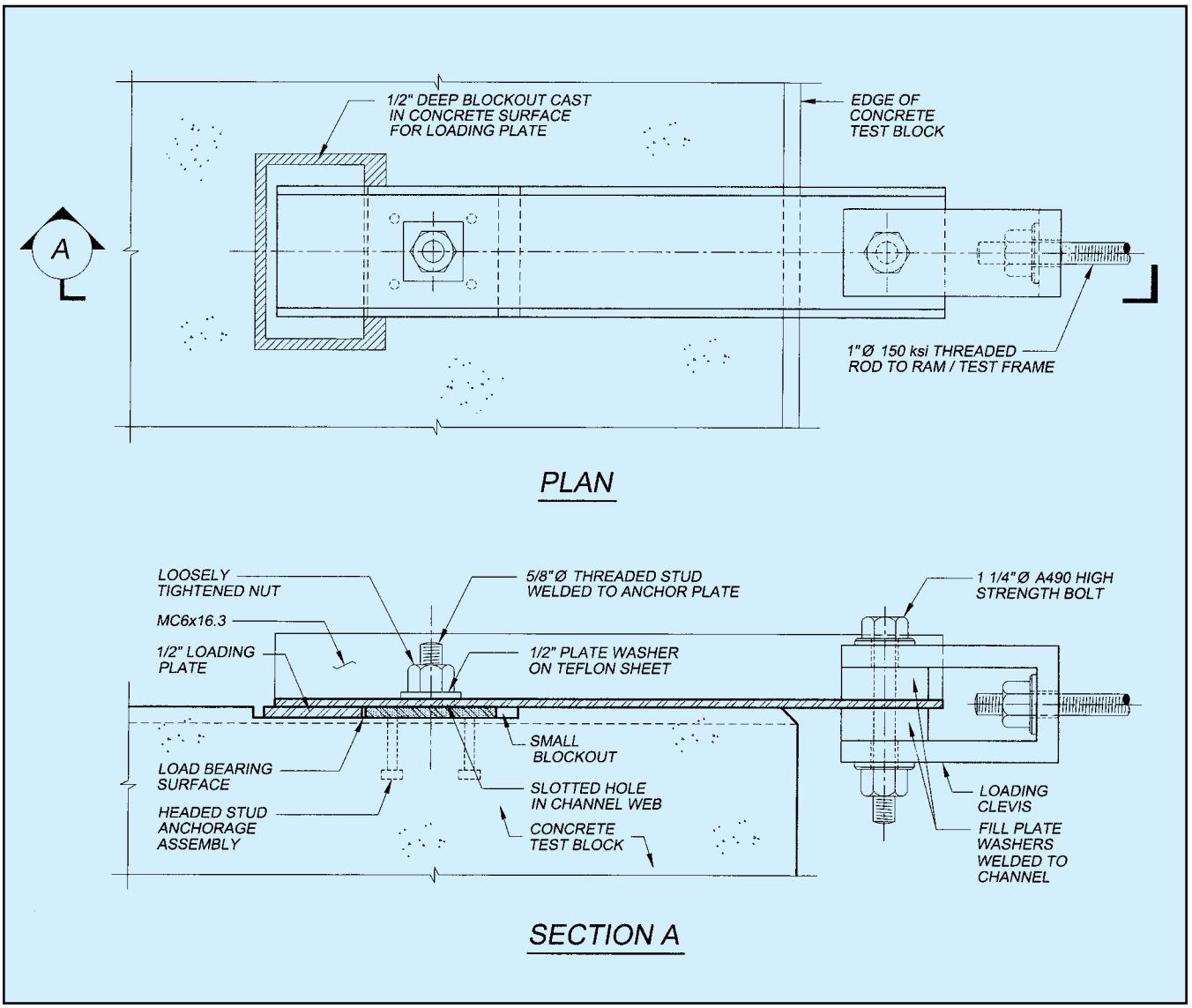

Fig. 10. Details of shoe for loading the embedded plate assembly.

loading, brought on by the testing setup, may have induced the concrete breakout observed in the pilot study. Consequently, a few test series were planned in this program to evaluate the back edge distance, de4.

In this study, 23 tests were conducted with the shear force applied away from the back free edge. This can be seen in Fig. 1, which shows the shear force direction and the definition of the de4 back edge distance. Three separate test series were evaluated; two series had single studs and the third series had two headed studs oriented in one *y*-row.

The two series of single stud anchorages examined both 1/2 and 5/8 in. (12.7 and 15.9 mm) diameter studs. The two stud anchorage groups used 1/2 in. (12.7 mm) diameter studs, spaced 2 1/4 in. (57.2 mm) or 4.5*d* apart. All three series were tested in 16 in. (406 mm) thick specimens. The test series identifications for the de4 tests are shown in Table 6. As shown in Table 6, h_{ef}/d ratios for these tests were 5.3 and 5.93.

Test Behavior

For the 1/2 in. diameter single stud connection (identified as Series V140_), five de4 edge distances were evaluated with two tests performed per edge distance. The five edge distances were nominally 4*d*, 6*d*, 8*d*, 10*d*, and 12*d*. Eight of these tests failed due to steel stud failure, and two failed in the weld to the plate. After failure in all cases, only minor concrete damage was observed. Crushing of the concrete in front of the stud was accompanied by hairline, transverse cracks (cracks perpendicular to the applied shear load) propagating 2 to 4 in. (51 to 102 mm) either side from the stud center.

Seven tests were conducted (identified as Series V141_) using 5/8 in. (15.9 mm) diameter studs. Edge distances evaluated were 4*d*, 8*d*, and 12*d*. Three tests were conducted at the closest edge distance of 4*d* or 2 1/2 in. (63.5 mm). All tests at the three edge distances failed in a steel shear mode, with no weld failures occurring in this series. Fig. 11 shows a representative test specimen, Test V1411B, following stud failure. Based on these test results, it was apparent that the back edge distance, de4, variable is not a factor that causes concrete breakout of

Table 6. Back edge distance (de4) test summary.

(1) Group information	(2) Test No.	(3) No. of studs (*n*)	(4) Front row (FR)	(5) Back row (BR)	(6) Side row (SR)	(7) Stud diameter *d* (in.)	(8) Embed depth h_{ef} (in.)	(9) Concrete strength f'_c (psi)	(10) Ratio h_{ef}/d	(11) Test geometry de3 (in.)	(12) Test geometry de4 (in.)	(13) de1 (in.)	(14) de2 (in.)	(15) *x* (in.)	(16) Primary ED factor (de4/d)	(17) V_{test} (kips)	(18) Stud strength F_u (ksi)	(19) Steel capacity (kips)	(20) Steel test/ pred	(21) Actual failure mode
V140_ Series	V1401A	1	1	0	1	0.494	2.63	6700	5.32	46.0	2.0	12.00	108.00	0	4.0	15.8	81.6	15.6	1.01	Stud
W-Stud	V1401B	1	1	0	0	1	0.494	2.63	6580	5.32	46.0	2.0	20.00	100.00	0	4.0	16.2	81.6	15.6	1.04
d = 1/2 in.	V1402A	1	1	0	1	0.494	2.63	6680	5.32	45.0	3.0	28.75	91.25	0	6.1	16.5	81.6	15.6	1.05	Stud
h_{ef} = 2.63 in.	V1402B	1	1	0	1	0.494	2.63	6680	5.32	45.0	3.0	40.75	79.25	0	6.1	15.8	81.6	15.6	1.01	Stud
h = 16 in.	V1403A	1	1	0	1	0.494	2.63	6680	5.32	44.0	4.0	54.75	65.25	0	8.1	17.6	81.6	15.6	1.13	Stud
	V1403B	1	1	0	1	0.494	2.63	6680	5.32	44.0	4.0	49.25	70.75	0	8.1	14.5	81.6	15.6	0.93	W-Stud
	V1404A	1	1	0	1	0.494	2.63	5690	5.32	43.0	5.0	18.75	101.25	0	10.1	17.1	81.6	15.6	1.09	Stud
	V1404B	1	1	0	1	0.494	2.63	5690	5.32	43.0	5.0	33.75	86.25	0	10.1	17.5	81.6	15.6	1.12	Stud
	V1405A	1	1	0	1	0.494	2.63	5700	5.32	42.0	6.0	50.25	69.75	0	12.1	17.4	81.6	15.6	1.11	Stud
	V1405B	1	1	0	1	0.494	2.63	5700	5.32	42.0	6.0	54.75	65.25	0	12.1	18.1	81.6	15.6	1.16	Stud
V141_ Series	V1411A	1	1	0	1	0.624	3.70	6580	5.93	45.5	2.5	20.00	100.00	0	4.0	22.8	78.0	23.9	0.96	Stud
	V1411B	1	1	0	0	1	0.624	3.70	6700	5.93	45.5	2.5	12.00	108.00	0	4.0	21.8	78.0	23.9	0.91
Stud$d$ = 5/8 in.	V1411C	1	1	0	1	0.624	3.70	6430	5.93	45.5	2.5	24.00	24.00	0	4.0	24.2	78.0	23.9	1.01	Stud
h_{ef} = 3.7 in.	V1412A	1	1	0	1	0.624	3.70	6470	5.93	43.0	5.0	32.25	36.00	0	8.0	26.8	78.0	23.9	1.12	Stud
h = 16 in.	V1412B	1	1	0	1	0.624	3.70	6470	5.93	43.0	5.0	17.25	36.00	0	8.0	25.5	78.0	23.9	1.07	Stud
	V1413A	1	1	0	1	0.624	3.70	5700	5.93	40.5	7.5	39.75	80.25	0	12.0	23.9	78.0	23.9	1.00	Stud
	V1413B	1	1	0	1	0.624	3.70	5700	5.93	40.5	7.5	24.75	95.25	0	12.0	24.1	78.0	23.9	1.01	Stud
V240_ Series	V2401A	2	2	0	1	0.496	2.63	6430	5.30	46.0	2.0	11.75	34.00	2.25	4.0	26.2	77.7	30.0	0.87	W-Stud
	V2401B	2	2	2	0	1	0.496	2.63	6430	5.30	46.0	2.0	34.00	11.75	2.25	4.0	27.0	77.7	30.0	0.90
Stud2 X-rows	V2402A	2	2	0	1	0.496	2.63	6700	5.30	44.0	4.0	32.00	85.75	2.25	8.1	30.9	77.7	30.0	1.03	Stud
x = 4.5d	V2402B	2	2	0	1	0.496	2.63	6470	5.30	44.0	4.0	45.75	72.00	2.25	8.1	31.2	77.7	30.0	1.04	Stud

Note: Test type = shear at de4 edge; number of anchors = 1 and 2; maximum aggr. size = 3/4 in., normal weigth concrete; slab thickness = 16 in.; Columns 11 to 15: refer to Fig. 1 for geometric notation; Column 16: ED = edge distance; Column 19: $V_s = A_s F_{ut}$ (predicted steel capacity); Column 21: stud = ductile failure of the steel stud and, W-Stud = stud weld failure; note: 1 in. = 25.4 mm; 1 kip = 4.448 kN; 1 psi = 6.895 kPa; 1 ksi = 6.895 MPa.

Fig. 11. Steel shear failure of $^5/_8$ in. (16 mm) diameter stud with a back edge distance (de4) of 4*d*.

Fig. 12. Local concrete crushing and steel shear failure of $^1/_2$ in. (12.7 mm) diameter studs with back edge distance (de4) of 8*d*.

single stud anchorages.

The two stud anchorage series (identified as Series V240_) used $^1/_2$ in. (12.7 mm) diameter studs at nominal edge distances of 4*d*, 8*d*, and 12*d*. Six total tests were conducted in this series. Two of the tests exhibited weld failures in one or both of the studs, while the other four tests failed by the stud shearing through both of the stud shanks.

Following failure, it was found that at these anchorage locations, only localized damage occurred to the concrete in the form of concrete crushing. Transverse splitting cracks were found to propagate from the studs but were arrested in a short distance. No concrete cracking propagated longitudinally to the back free edge, even after isopropyl alcohol was used to visually aid in tracking cracks.

Fig. 12 shows a typical steel stud failure for the two-stud anchorage loaded away from the back free edge. It is important to note that there was no supplementary reinforcement around or near any of these anchorages.

Table 6, Column 17, presents the failure loads for all of these tests. Because steel failure dominated the failure mode, the test loads are evaluated based on a steel capacity predicted using 1.0 A_sF_{ut}. Column 19 lists the predicted steel capacity and Column 20 shows the test-to-predicted ratio for the tests.

The test-to-predicted capacities for a majority of the stud failures are generally above 1.0. Tests V1411A, V1411B, and V2401B, which were

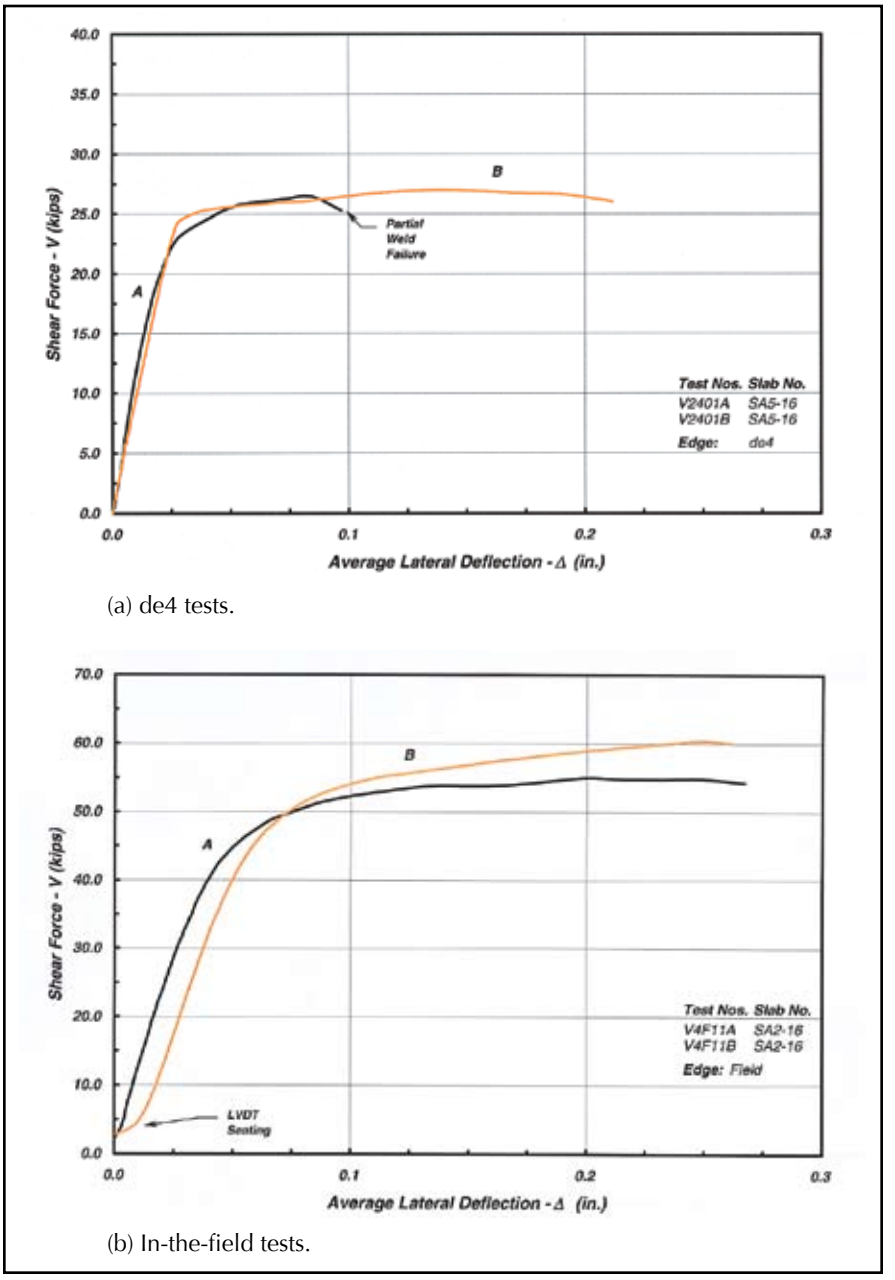

(a) de4 tests.

(b) In-the-field tests.

Fig. 13. Load-deformation behavior for steel failure.

Table 7. In-the-field test summary.

(1)	(2)	(3)	(4)	(5)	(6)	(7)	(8)	(9)	(10)	(11)	(12)	(13)	(14)	(15)	(16)	(17)	(18)	(19)	(20)	(21)	(22)	(23)
										Test geometry						ED Factors						
Group information	Test no.	No. of studs (n)	Front row (FR)	Back row (BR)	Side row (SR)	Stud dia. d (in.)	Embed depth h_{ef} (in.)	Concrete strength f'_c (psi)	Ratio h_{ef}/d	de3 (in.)	de4 (in.)	de1 (in.)	de2 (in.)	x (in.)	y (in.)	Primary de3/d	Secondary [de3+y]/d	V_{test} (kips)	Stud strength F_u (ksi)	Steel capacity (kips)	Steel test/ Pred	Actual failure mode
V2F0_	V2F01A	2	2	0	1	0.496	2.63	6450	5.30	32.00	16.00	15.00	30.75	2.25	0.00	64.5	64.5	29.4	77.7	30.0	0.98	Stud
Series	V2F01B	2	2	0	1	0.496	2.63	6450	5.30	32.00	16.00	30.75	15.00	2.25	0.00	64.5	64.5	31.4	77.7	30.0	1.05	Stud
2 X-rows	V2F02A	2	2	0	1	0.495	4.87	6580	9.84	30.00	18.00	35.75	82.00.	2.25	0.00	60.6	60.6	30.0	79.1	30.4	0.99	W-Stud
$x = 4.5d$	V2F02B	2	2	0	1	0.495	4.87	6700	9.84	30.00	18.00	50.00	67.75	2.25	0.00	60.6	60.6	26.5	79.1	30.4	0.87	W-Stud
V2F1_	V2F11A	2	2	0	1	0.496	2.63	6700	5.30	30.00	18.00	20.25	96.25	3.50	0.00	60.5	60.5	29.1	77.7	30.0	0.97	Stud
Series	V2F11B	2	2	0	1	0.496	2.63	6700	5.30	18.00	30.00	27.25	89.25	3.50	0.00	36.3	36.3	29.1	77.7	30.0	0.97	Stud
2 X-rows	V2F12A	2	2	0	1	0.495	4.87	6700	9.84	18.00	30.00	42.75	77.25	3.50	0.00	36.4	36.4	29.1	79.1	30.4	0.96	Stud
$x = 7.0d$	V2F12B	2	2	0	1	0.495	4.87	6580	9.84	18.00	30.00	58.25	61.75	3.50	0.00	36.4	36.4	27.2	79.1	30.4	0.89	W-Stud
V2F2_	V2F21A	2	1	1	2	0.496	2.63	6580	5.30	28.88	16.88	67.75	52.25	0.00	2.25	58.2	62.8	30.9	77.7	30.0	1.03	Stud
Series	V2F21B	2	1	1	2	0.496	2.63	6700	5.30	28.88	16.88	79.75	40.25	0.00	2.25	58.2	62.8	29.0	77.7	30.0	0.97	Stud
2 Y-rows	V2F22A	2	1	1	2	0.495	4.87	6700	9.84	28.88	16.88	91.75	28.25	0.00	2.25	58.3	62.9	32.0	79.1	30.4	1.05	Stud
$y = 4.5d$	V2F22B	2	1	1	2	0.495	4.87	6700	9.84	28.88	16.88	103.75	16.25	0.00	2.25	58.3	62.9	30.6	79.1	30.4	1.01	Stud
V2F3_	V2F31A	2	1	1	2	0.496	2.63	6580	5.30	16.25	28.25	46.25	73.75	0.00	3.50	32.8	39.8	30.6	77.7	30.0	1.02	Stud
Series	V2F31B	2	1	1	2	0.496	2.63	6700	5.30	16.25	28.25	34.25	85.75	0.00	3.50	32.8	39.8	27.6	77.7	30.0	0.92	Stud
2 Y-rows	V2F32A	2	1	1	2	0.495	4.87	6700	9.84	16.25	28.25	22.25	97.75	0.00	3.50	32.8	39.9	30.5	79.1	30.4	1.00	Stud
$y = 7.0d$	V2F32B	2	1	1	2	0.495	4.87	6490	9.84	22.25	22.25	19.50	100.50	0.00	3.50	44.9	52.0	30.0	79.1	30.4	0.99	Stud
V4F0_	V4F01A	4	2	2	2	0.496	2.63	5160	5.30	38.25	19.50	18.00	39.75	2.25	2.25	77.1	81.7	54.7	77.7	60.1	0.91	Stud
Series	V4F01B	4	2	2	2	0.496	2.63	6570	5.30	30.00	15.75	55.75	62.00	2.25	2.25	60.5	65.0	58.7	77.7	60.1	0.98	Stud
2 X and Y	V4F02C	4	2	2	2	0.495	4.87	5160	9.84	38.25	19.50	21.75	36.00	2.25	2.25	77.3	81.8	58.3	79.1	60.9	0.96	Stud
	rows	V4F02D	4	2	2	2	0.495	4.87	5160	9.84	38.25	19.50	21.75	36.00	2.25	2.25	77.3	81.8	54.6	79.1	60.9	0.90	Stud
$x = y = 4.5d$																						
V4F1_	V4F11A	4	2	2	2	0.496	2.63	6570	5.30	30.00	14.50	45.75	72.00	2.25	3.50	60.5	67.5	55.0	77.7	60.1	0.92	Stud

Note: Number of tests = 24; Columns 11 to 16 refer to Fig. 1 for geometric notation; Columns 17 and 18 ED = edge distance; Column 21 $V_s = A_s F_{ut}$ (predicted steel capacity); Column 23 stud = ductile failure of the steel stud and W-Stud = stud weld failure; note: 1 in. = 25.4 mm; 1 kip = 4.448 kN; 1 psi = 6.895 kPa; 1 ksi = 6.895 MPa.

Table 8. Steel failure test results.

(1) Test number	(2) Test type (edge)	(3) Number of studs (n)	(4) Stud diameter d (in.)	(5) Tensile stress F_{ut} (ksi)	(6) Steel capacity (kips)	(7) Failure load (kips)	(8) Test/ predict (actual)	(9) Test/ predict (design)	(10) Failure type
V1102B	de1	1	0.494	81.6	15.6	16.1	1.03	1.29	Stud
V1103A	de1	1	0.494	81.6	15.6	16.1	1.03	1.29	Stud
V1103B	de1	1	0.494	81.6	15.6	14.3	0.91	1.15	Stud
V1111B	de1	1	0.624	78.0	23.9	22.6	0.95	1.14	Stud
V1112A	de1	1	0.624	78.0	23.9	25.6	1.07	1.29	Stud
V1112B	de1	1	0.624	78.0	23.9	24.5	1.03	1.23	Stud
V1113A	de1	1	0.624	78.0	23.9	22.8	0.96	1.15	Stud
V1113B	de1	1	0.624	78.0	23.9	25.1	1.05	1.26	Stud
V1122A	de1	1	0.495	79.1	15.2	14.3	0.94	1.14	Stud
V1122B	de1	1	0.495	79.1	15.2	14.5	0.95	1.16	Stud
V1152A	de1	1	0.494	81.6	15.6	15.0	0.96	1.20	Stud
V1152B	de1	1	0.494	81.6	15.6	15.8	1.01	1.27	Stud
V1153B	de1	1	0.494	81.6	15.6	18.2	1.16	1.46	Stud
V1163A	de1	1	0.624	78.0	23.9	25.0	1.05	1.26	Stud
V2102A	de1	2	0.496	77.7	30.0	28.1	0.94	1.12	Stud
V2103A	de1	2	0.496	77.7	30.0	30.4	1.01	1.21	Stud
V2111A	de1	2	0.496	77.7	30.0	30.1	1.00	1.20	Stud
V2111B	de1	2	0.496	77.7	30.0	27.7	0.92	1.10	Stud
V2124A	de1	2	0.496	81.6	31.5	27.5	0.87	1.09	Stud
V2124B	de1	2	0.496	81.6	31.5	27.6	0.88	1.10	Stud
V2161A	de1	2	0.496	77.7	30.0	30.4	1.01	1.21	Stud
V2161B	de1	2	0.496	77.7	30.0	28.5	0.95	1.13	Stud
V2174A	de1	2	0.496	77.7	30.0	29.9	1.00	1.19	Stud
V2174B	de1	2	0.496	77.7	30.0	28.4	0.95	1.13	Stud
V3174A	de1	3	0.496	77.7	45.0	38.1	0.85	1.01	Stud
V1303A	de3	1	0.494	81.6	15.6	17.0	1.09	1.36	Stud
V1303A	de3	1	0.494	81.6	15.6	17.5	1.12	1.40	Stud
V1313A	de3	1	0.624	78.0	23.9	25.3	1.06	1.27	Stud
V1314A	de3	1	0.624	78.0	23.9	24.9	1.04	1.25	Stud
V1323B	de3	1	0.495	79.1	15.2	16.3	1.07	1.30	Stud
V1323C	de3	1	0.495	79.1	15.2	16.7	1.10	1.34	Stud
V2324A	de3	2	0.496	77.7	30.0	28.3	0.94	1.13	Stud
V2324B	de3	2	0.496	77.7	30.0	29.0	0.97	1.15	Stud
V2334A	de3	2	0.496	81.6	31.5	28.3	0.90	1.13	Stud
V2334B	de3	2	0.496	81.6	31.5	30.7	0.97	1.22	Stud
V2335A	de3	2	0.496	81.6	31.5	28.7	0.91	1.14	Stud
V1401A	de4	1	0.494	81.6	15.6	15.8	1.01	1.27	Stud
V1402A	de4	1	0.494	81.6	15.6	16.5	1.05	1.32	Stud
V1402B	de4	1	0.494	81.6	15.6	15.8	1.01	1.27	Stud
V1403A	de4	1	0.494	81.6	15.6	17.6	1.13	1.41	Stud
V1404A	de4	1	0.494	81.6	15.6	17.1	1.09	1.37	Stud
V1404B	de4	1	0.494	81.6	15.6	17.5	1.12	1.40	Stud
V1405A	de4	1	0.494	81.6	15.6	17.4	1.11	1.40	Stud
V1405B	de4	1	0.494	81.6	15.6	18.1	1.16	1.45	Stud
V1411A	de4	1	0.624	78.0	23.9	22.8	0.96	1.15	Stud
V1411B	de4	1	0.624	78.0	23.9	21.8	0.91	1.10	Stud
V1411C	de4	1	0.624	78.0	23.9	24.2	1.01	1.22	Stud
V1412A	de4	1	0.624	78.0	23.9	26.8	1.12	1.35	Stud
V1412B	de4	1	0.624	78.0	23.9	25.5	1.07	1.28	Stud
V1413A	de4	1	0.624	78.0	23.9	23.9	1.00	1.20	Stud
V1413B	de4	1	0.624	78.0	23.9	24.1	1.01	1.21	Stud
V2401B	de4	2	0.496	77.7	30.0	27.0	0.90	1.07	Stud
V2402A	de4	2	0.496	77.7	30.0	30.9	1.03	1.23	Stud

Note: Column 6: $V_s = A_s F_{ut}$ (steel capacity); Column 8: F_{ut} = actual from Column 5; Column 9: F_{ut} = 65 ksi (minimum design from Table 3); Column 10: stud = ductile failure of the steel stud; W-stud = stud weld failure; note: 1 in. = 25.4 mm; 1 kip = 4.448 kN; 1 ksi = 6.895 MPa.

Table 8. (cont.). Steel failure test results.

(1) Test number	(2) Test type (edge)	(3) Number of studs (n)	(4) Stud diameter d (in.)	(5) Tensile stress F_{ut} (ksi)	(6) Steel capacity (kips)	(7) Failure load (kips)	(8) Test/ predict (actual)	(9) Test/ predict (design)	(10) Failure type
V2F01A	Field	2	0.496	77.7	30.0	29.4	0.98	1.17	Stud
V2F01B	Field	2	0.496	77.7	30.0	31.4	1.05	1.25	Stud
V2F11A	Field	2	0.496	77.7	30.0	29.1	0.97	1.16	Stud
V2F11B	Field	2	0.496	77.7	30.0	29.1	0.97	1.16	Stud
V2F12A	Field	2	0.495	79.1	30.4	29.1	0.96	1.16	Stud
V2F21A	Field	2	0.496	77.7	30.0	30.9	1.03	1.23	Stud
V2F21B	Field	2	0.496	77.7	30.0	29.0	0.97	1.15	Stud
V2F22A	Field	2	0.495	79.1	30.4	32.0	1.05	1.28	Stud
V2F22B	Field	2	0.495	79.1	30.4	30.6	1.01	1.22	Stud
V2F31A	Field	2	0.496	77.7	30.0	30.6	1.02	1.22	Stud
V2F31B	Field	2	0.496	77.7	30.0	27.6	0.92	1.10	Stud
V2F32A	Field	2	0.495	79.1	30.4	30.5	1.00	1.22	Stud
V2F32B	Field	2	0.495	79.1	30.4	30.0	0.99	1.20	Stud
V4F01A	Field	4	0.496	77.7	60.1	54.7	0.91	1.09	Stud
V4F01B	Field	4	0.496	77.7	60.1	58.7	0.98	1.17	Stud
V4F02C	Field	4	0.495	79.1	60.9	58.3	0.96	1.17	Stud
V4F02D	Field	4	0.495	79.1	60.9	54.6	0.90	1.09	Stud
V4F11A	Field	4	0.496	77.7	60.1	55.0	0.92	1.09	Stud
V4F11B	Field	4	0.496	77.7	60.1	60.4	1.01	1.20	Stud
V4F12A	Field	4	0.495	79.1	60.9	60.1	0.99	1.20	Stud
V4F12B	Field	4	0.495	79.1	60.9	57.8	0.95	1.16	Stud
PO12-10	Push-Off	6	0.494	82.4	94.7	84.7	0.89	1.13	Stud
PO12-7	Push-Off	6	0.494	82.4	94.7	84.1	0.89	1.13	Stud
PO12-8	Push-Off	6	0.494	82.4	94.7	86.5	0.91	1.16	Stud
PO12-9	Push-Off	6	0.494	82.4	94.7	96.6	1.02	1.29	Stud
V1101A	de1	1	0.494	81.6	15.6	10.8	0.69	0.87	W-Stud
V1102A	de1	1	0.494	81.6	15.6	12.2	0.78	0.98	W-Stud
V1121A	de1	1	0.495	79.1	15.2	10.1	0.66	0.81	W-Stud
V1153A	de1	1	0.494	81.6	15.6	14.0	0.90	1.12	W-Stud
V2102B	de1	2	0.496	77.7	30.0	28.3	0.94	1.13	W-Stud
V3173A	de1	3	0.496	77.7	45.0	27.4	0.61	0.73	W-Stud
V2325A	de3	2	0.496	77.7	30.0	22.8	0.76	0.91	W-Stud
V2325B	de3	2	0.496	77.7	30.0	24.0	0.80	0.96	W-Stud
V2335B	de3	2	0.496	81.6	31.5	27.4	0.87	1.09	W-Stud
V2375B	de3	2	0.496	81.6	31.5	18.6	0.59	0.74	W-Stud
V1401B	de4	1	0.494	81.6	15.6	16.2	1.04	1.30	W-Stud
V1403B	de4	1	0.494	81.6	15.6	14.5	0.93	1.16	W-Stud
V2401A	de4	2	0.496	77.7	30.0	26.2	0.87	1.04	W-Stud
V2403B	de4	2	0.496	77.7	30.0	29.7	0.99	1.18	W-Stud
V2F02A	Field	2	0.495	79.1	30.4	30.0	0.99	1.20	W-Stud
V2F02B	Field	2	0.495	79.1	30.4	26.5	0.87	1.06	W-Stud

Note: Column 6: $V_s = A_s F_{ut}$ (steel capacity); Column 8: F_{ut} = actual from Column 5; Column 9: F_{ut} = 65 ksi (minimum design from Table 3); Column 10: stud = ductile failure of the steel stud; W-stud = stud weld failure; note: 1 in. = 25.4 mm; 1 kip = 4.448 kN; 1 ksi = 6.895 MPa.

categorized as stud shear failures, exhibited lower test-to-predicted capacities of 0.90 to 0.96. A review of the photograph for Test V2401B showed a potential weldment problem in one of the two studs. In assessing the weldment after failure, it did not exhibit significant enough porosity (air voids) to classify it as a weld failure.

The four weld failures encountered in this test series also exhibited a unique but variable behavior. Two of the weld failures had test-to-predicted capacities of 0.87 and 0.93; however, the two remaining "weld failures" had test-to-predicted capacities approximately equal to 1.0. Evidence of porosity was observed within the circumference of the weld; however, this porosity appears to have had minimal influence on the connection capacity when compared to 1.0 $A_s F_{ut}$.

Fig. 13(a) shows two representative load-deformation curves for the two anchor tests. Test V2401A was found to exhibit a partial weld failure as discussed above and failed in a more brittle manner, but only after achieving about 0.1 in. (2.5 mm) of deformation. Companion Test V2401B was a stud shearing failure. As shown in Fig. 13(a), this test showed good ductile behavior.

TESTS-IN-THE-FIELD

Some anchorages used in precast concrete members are located a sufficiently large distance away from all

edges that all concrete breakout capacities are in excess of the capacity that can develop by the individual studs failing in steel shearing. This series of testing was classified as in-the-field tests. Six test series were planned and tested in this program to test two- and four-anchor connections. For these six series, the emphasis was on evaluating if the *x*- and *y*-row spacing had an effect on capacity and if stud embedment depth had an influence.

This portion of the overall test program had 24 total tests. Each test series used 1/2 in. (12.7 mm) diameter studs. Two tests in the series used studs with an effective embedment depth (h_{ef}) of 2.69 in. (67.7 mm). Longer studs having an h_{ef} = 4.87 in. (124 mm) were used for the second two tests in the series.

All 24 tests were conducted on 16 in. (406 mm) thick test slab specimens. Based on previous push-off testing, discussed earlier, steel stud failure can be achieved in relatively thin slabs. As such, the influence of slab thickness on the ability of an anchorage to develop steel failure was viewed to have little effect, especially with the 1/2 in. (12.7 mm) diameter studs used in this study. The test series identifications relevant to the in-the-field tests are shown in Table-7.

Test Behavior

Of the 24 tests conducted in the six in-the-field test series, three of the anchorages failed by fracture in the stud weld. In a multi-stud anchorage, typically one of the stud welds failed. However, the entire anchorage was classified as a weld failure.

Weld failures were found to occur in the two stud anchorages evaluating *x*-spacing effects. Review of these weld failures showed two of the anchorages failing at a test-to-predicted ratio less than 0.90. The remaining weld failure, Test V2F02A, showed a test-to-predicted ratio of 0.99.

This test also showed good deformation behavior prior to failure. Moreover, the stud weld failure surface was marked by only minor porosity, estimated to be about 10 percent of the stud cross-sectional area. Therefore, this test can be considered as a steel failure, even though some weld failure tendencies were observed. Fig. 13(b) shows representative load-deformation curves of two tests that sheared the stud shank.

The test-to-predicted steel stud shear capacities, in Table 7, ranged from 0.90 to 1.05 for the six series of tests examined in the in-the-field testing. When the long stud results are compared with the short stud results for all series, there is no discernable increase or decrease in the ultimate steel shear capacity due to stud length.

With respect to stud spacing in the two-stud connection, the test-to-predicted capacity ratios are within 4 to 5 percent of each other, within the expected scatter for the stud strength data (discussed in the following section). The data in Table 7 show the variation of the capacity with *x*- and *y*-spacing as the variable. Because of the limited amount of data, the authors believe that these results reflect the normal scatter in steel strength rather than an influence of spacing.

For the four-stud connection, the average test-to-predicted capacity of the connection having a larger *y*-spacing ($y = 7.0d$) is greater than those with a smaller *y*-spacing of 4.5*d*. The capacity ratio for the two series are within 3 percent, which is again considered to be within the scatter of the strength of the stud material.

In summary, it appears that *x*- or *y*-spacings of 4.5*d* and 7.0*d* in different combinations and loading orientations did not have a significant effect on the ultimate steel strength of the given connection. Mean test-to-predicted steel capacities ranged from 0.93 to 1.03 for the six-series.

STEEL FAILURE ANALYSIS

As discussed in the previous sections, a failure mode governed by steel stud failure typically occurred for back edge (de4) and in-the-field tests performed in 16 in. (406 mm) thick slabs. Approximately one-half of the database from this program on steel shear failures is based on the de4 and in-the-field testing. Additionally, steel failures were obtained in the side edge (de1) and front edge distance (de3) testing.

Steel failures, in these other two testing regimes, occurred when the edge distance was large enough to transition from concrete breakout to steel stud shear failure. Those steel shear failures are compiled with the other de4 and in-the-field tests resulting in a shear strength steel capacity database of 97 total tests, shown in Table-8.

In all cases, steel failures were typically marked by two failure modes: a ductile, yielding-type failure of the stud or a stud weld failure at the plate interface. Ductile failures were accompanied by appreciable lateral deformation. Figs. 13(a) and 13(b) showed representative load-deflection curves of a ductile steel shear failure of the stud.

These figures illustrate that post-elastic yielding in shear exists, as evidenced by the flat topped portion of the plot. After fracture, the stud failure surface exhibited a shear yielding-type

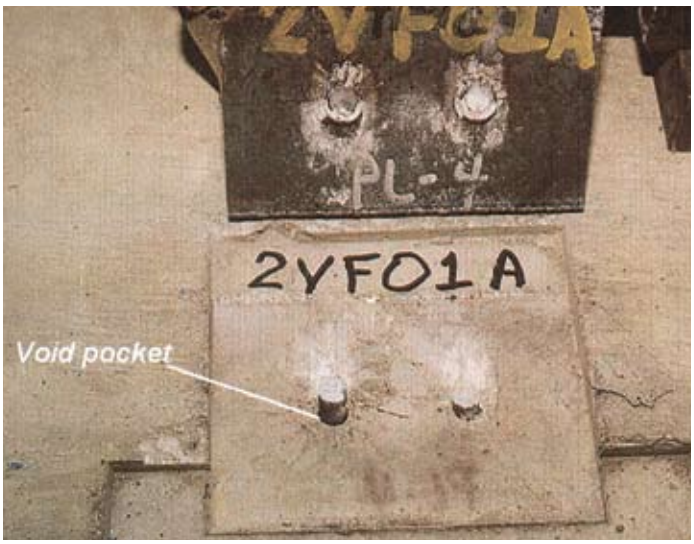

Fig. 14. Shear failure of stud shank with local crushing of concrete.

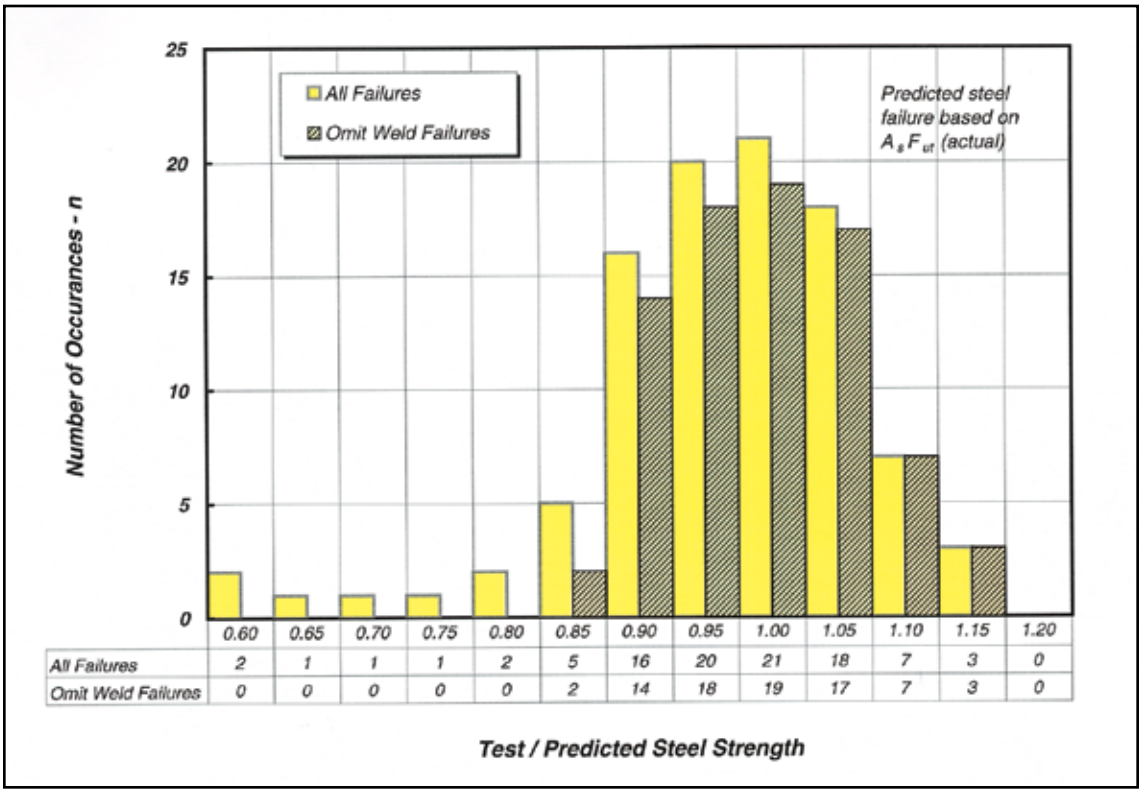

	0.60	0.65	0.70	0.75	0.80	0.85	0.90	0.95	1.00	1.05	1.10	1.15	1.20
All Failures	2	1	1	1	2	5	16	20	21	18	7	3	0
Omit Weld Failures	0	0	0	0	0	2	14	18	19	17	7	3	0

Fig. 15(a). Histogram showing the distribution of steel failure data with actual ultimate tensile strength.

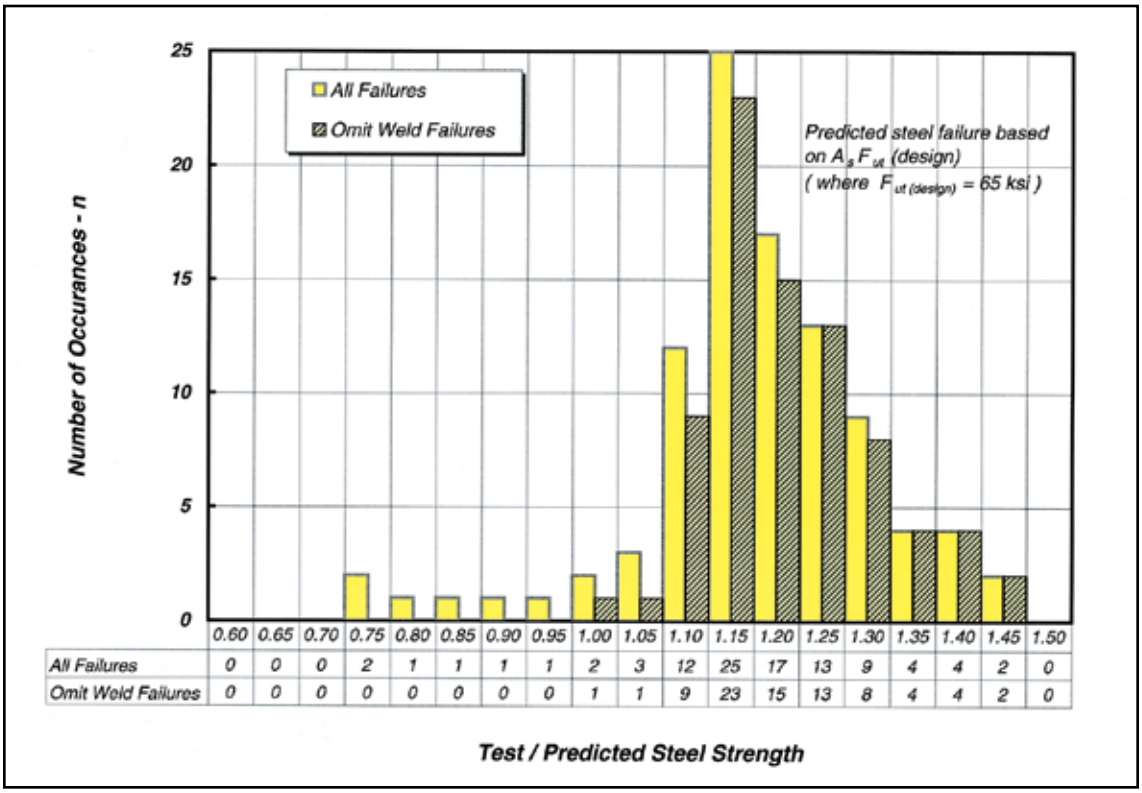

	0.60	0.65	0.70	0.75	0.80	0.85	0.90	0.95	1.00	1.05	1.10	1.15	1.20	1.25	1.30	1.35	1.40	1.45	1.50
All Failures	0	0	0	2	1	1	1	1	2	3	12	25	17	13	9	4	4	2	0
Omit Weld Failures	0	0	0	0	0	0	0	0	1	1	9	23	15	13	8	4	4	2	0

Fig. 15(b). Histogram showing the distribution of steel failure data with minimum design tensile strength.

profile indicative of good ductile behavior. This is opposed to a failure surface marked by porosity from inadequate weld fusion. The ductile failure surface was generally located in the stud shank directly adjacent to the weld flash.

When the corresponding failure area on the concrete slab specimen was observed, the still embedded studs had fracture surfaces that were elliptical-shaped in plan with the major axis parallel to the load direction. The concrete bearing surface in front of the stud was locally crushed, with a "powdery" appearance. Also, because of the elliptical nature of the stud failure surface and associated lateral deformation, a void (pocket) behind the stud was created; this void represented the former location of the stud when the concrete

was cast.

An example of this classical failure mode is illustrated in Fig. 14. As shown in this figure, transverse cracks perpendicular to the applied shear load propagated from the concrete crushing zone. These cracks were typically quite shallow and were representative of the stress state in the concrete just prior to failure.

The second steel failure type experienced was failure of the stud weld to the plate. Varying degrees of porosity in the weld region confined within the shank diameter typically marked the weld failure surface. Porosity amounts often ranged from 25 to 75 percent of the shank area.

For this test program, the stud failures due to welding appeared to be a random occurrence. As an example, WJE tested numerous multi-stud anchorage plate configurations. In most instances, only one of the studs in a multi-stud anchorage would experience a weld failure, whereas the remaining studs appeared to have adequate welds because they failed by shearing the stud shank. On any given multi-stud connection plate, the studs used were exactly the same, and the settings on the stud-welding machine remained unchanged, confirming the apparent randomness of the weld failure.

Failure load achieved for an anchorage governed by steel stud shank failure can typically be predicted using the ultimate tensile strength of the stud. In other words, the connection shear strength can be calculated by the number of studs times the stud area multiplied by the ultimate tensile strength of the material. Weld failures typically occurred at steel stresses less than the ultimate tensile strength.

All Steel Failures

WJE reviewed the steel shear failure data by first evaluating the actual tensile strength of the stud material. Ultimate tensile stresses were obtained for each stud heat and stud size, as reported earlier. WJE then compared the calculated A_sF_{ut} strength to the actual test failure load in shear, as shown in Column-8 of Table-8. Fig. 15(a) presents a histogram of all the steel failures, with all steel failures shown as solid bars.

For the 97 tests representing all steel failures (steel shank and weldment), WJE obtained an average test-to-predicted ratio of 0.967 and a standard deviation of 0.105 as presented in Table 9. The variance for this sample is 0.011 and the coefficient of variation (COV) is 10.8-percent. These statistics include weld failures in the database. When the data are analyzed for the 5 percent fractile value using a 90 percent confidence level, one obtains a κ factor of 1.95 for the population of 97 samples.

Using the probability distribution information, summarized by Wollmershauser,[34] the 5-percent fractile value is 0.76. Thus, for all of the non-concrete break-out failures, WJE data indicates the characteristic steel capacity, using the actual steel tensile strength, can be predicted by the following formula:

$$V_{steel} = 0.76\, A_s F_{ut(actual)} \quad (3a)$$

where

V_{steel} = nominal shear strength of a single headed stud or group of headed studs governed by steel strength (lb)

A_s = effective cross-sectional area of a stud anchor (sq in.)

$F_{ut(actual)}$ = actual ultimate tensile strength of headed stud steel in tension (psi)

The above value was obtained using the actual ultimate tensile strength (F_{ut}) of the headed stud steel. When the connection capacity is predicted using the design steel ultimate strength value of 65 ksi (450 MPa), the test-to-predicted ratio averages 1.18 with a standard deviation of 0.132. The variance is 0.017 and the COV is 11.2 percent. Therefore, the design equation for all steel failures using a design minimum F_{ut} = 65 ksi (450 MPa) reduced for the 5-percent fractile value becomes:

$$V_{steel(design)} = 0.92\, A_s F_{ut(design)} \quad (3b)$$

where

$V_{steel(design)}$ = nominal shear strength of a single headed stud or group of headed studs governed by steel strength (lb)

A_s = effective cross-sectional area of a stud anchor (sq in.)

$F_{ut\ (design)}$ = design minimum tensile strength of headed stud steel in tension, per Table 3 (psi)

A histogram of test-to-predicted ratios using the design ultimate steel strength is presented in Fig. 15(b). Given that the minimum design value of 65 ksi (450 MPa) ranges from 16 to 20-percent lower than the actual mea-

Table 9. Steel test-to-predicted statistics using actual ultimate and design tensile strengths of the studs.

	All failures		Stud failures only	
Statistic	Test F_{ut} = actual value	Design F_{ut} (min) = 65 ksi	Test F_{ut} = actual value	Design F_{ut} (min) = 65 ksi
Weld failures	17	17	0	0
Total tests	97	97	80	80
Average	0.97	1.18	1.00	1.21
Median	0.98	1.18	1.00	1.20
Standard deviation	0.105	0.132	0.071	0.095
Variance	0.011	0.017	0.005	0.009
COV	10.8 percent	11.2 percent	7.1 percent	7.8 percent
κ factor	1.95	1.95	1.96	1.96
5 percent fractile value	0.76	0.92	0.86	1.03

Note: 1 ksi = 6.895 MPa.

sured ultimate strength values of studs used in this program, a right shift in the Fig. 15(b) histogram is observed. Moreover, only six of the tests showed test-to-predicted ratios less than one by this analysis.

Steel Shank Failures Only

When the weld failure data are omitted from the population, the WJE database is representative of stud steel shear failures only. When this database is independently reviewed, the total test population becomes 80 with an average test-to-predicted ratio of 0.996 as shown in Table 9. The standard deviation on this sample is 0.071, thus indicating the relative tightness of the data.

Furthermore, the variance is 0.005 and the COV is 7.1 percent. This data set is illustrated in Fig. 15(a) as cross-hatched bars; a right shift in these data can be observed relative to the data base with all steel failures. In this distribution, the data are also grouped tighter about the mean.

Given the data base of steel stud shank shear failure, the κ factor for the 5 percent fractile analysis increases slightly to 1.957. Given this value, the characteristic strength prediction equation when the ultimate tensile strength is known becomes:

$$V_{steel} = 0.86\, A_s F_{ut(actual)} \qquad (4a)$$

By examining only the stud steel failures, the 5 percent fractile value increases by 13 percent over Eq. (3a). A further increase is observed when the minimum design ultimate strength of 65 ksi (450 MPa) is used to analyze the data. By using the design ultimate strength, the average test-to-predicted ratio is 1.21 with a standard deviation of 0.095. The variance for this analysis is 0.009 and the COV is 7.8 percent. The 5 percent fractile characteristic prediction equation thus becomes:

$$V_{steel(design)} = 1.0\, A_s F_{ut(design)} \qquad (4b)$$

In this case, the 5 percent fractile coefficient actually exceeds 1.0, so 1.0 becomes the default maximum value. From a probability standpoint, this indicates with 90 percent confidence that over 95 percent of the failure loads occur at a value represented by Eq. (4b) above, using the minimum design ultimate steel strength of 65 ksi (450 MPa). From the histogram shown in Fig. 15(b), no tests had test-to-predicted ratios less than 1.0, using the WJE data.

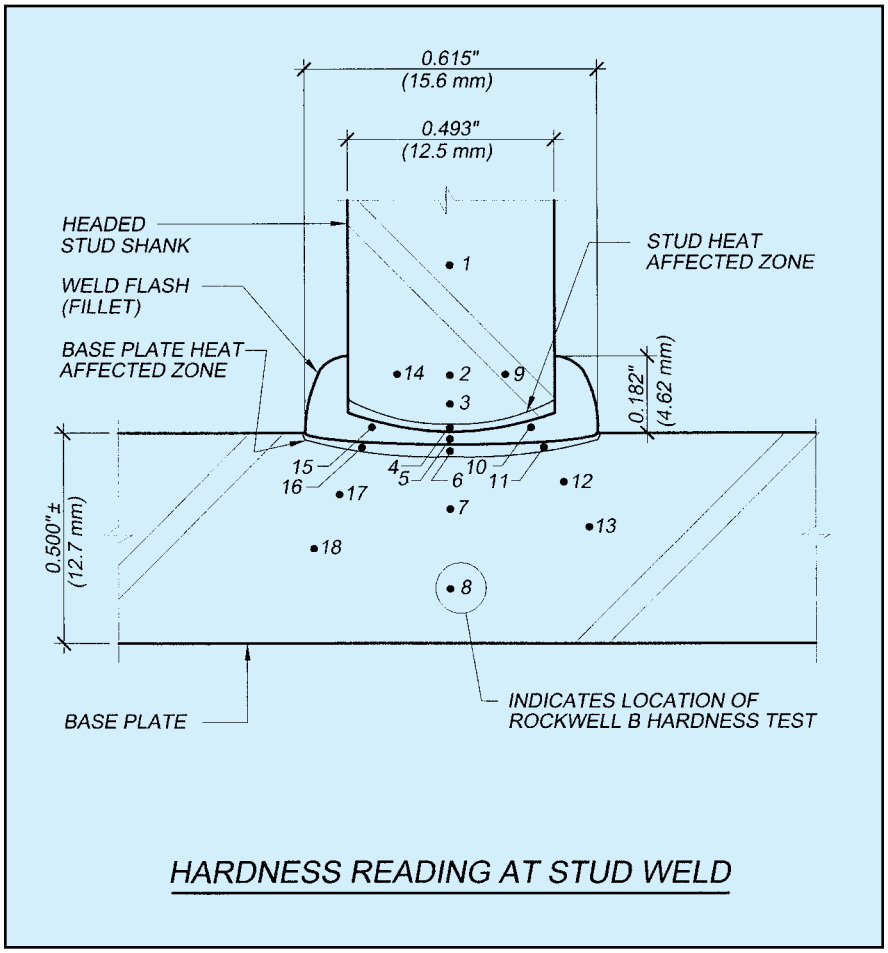

Fig. 16. Cross section of a stud shank, weld zone and anchorage plate showing hardness results.

Steel Failure Behavior

An explanation of the apparent increase in the steel shear strength when embedded in normal weight concrete, as compared to the shear strength results in air, can be founded in the metallurgy of the stud weld metal. In the stud welding process, the shielded arc weld melts the stud end and a shallow weld pool is created beneath the stud. The stud gun plunges the stud into the molten weld metal and holds the stud in position while the liquid metal solidifies. Although this process occurs over a very short period of time, a heat-affected zone (HAZ) is created in the weldment.

The American Welding Society defines the HAZ as that portion of the base metal where the mechanical properties or microstructure have been influenced by the heat of welding. The heat developed tends to heat-treat or temper the steel such that locally the steel's strength and hardness will increase. This transformation hardening process is dependent on the initial material temperature after arcing, the rate of cooling, and the final (ambient) temperature.[35]

Fig. 16 shows a cross section of a stud weld from this PCI research program. The anchorage, which in this case failed by a concrete breakout mode, was submitted to Nelson Stud Welding for metallurgical work.[36] The numbers on the cross section are locations where Rockwell B Hardness tests were performed on the weld and base metal cross section; the locations are shown in scale. The Rockwell B Hardness values were then approximately related back to ultimate tensile strength of the respective material.[37]

As shown in Table 10, the approximate tensile strengths are greater in the HAZ and immediate surrounding vicinity. Although a conversion of hardness to tensile strength is an approximation, the purpose herein is to show the relative steel strength increase in the weld area.

In relating Fig. 16 to the steel shear failures encountered in this study, the stud typically sheared off above the weld flash region in the parent stud material. Hardness locations 2, 9, and 14 in Fig. 16 exhibit converted tensile strengths of 96, 84, and 97.6 ksi (662, 579, and 673-MPa), respectively. Earlier tensile testing of this particular stud heat presented in Table 4, revealed an average ultimate tensile strength (F_{ut}) of 78 ksi (538 MPa). Therefore, on a relative basis, the indicated tensile strength in the area of the weld is between 10 to 20 ksi (60 to 138-MPa) higher.

Table 10. Rockwell B Hardness and equivalent tensile strengths of the stud weld area (see Fig. 16).

Hardness test location	Rockwell B hardness	Tensile strength (ksi)
1	90.1	88.0
2	93.5	96.0
3	91.8	92.0
4	95.1	102.0
5	101.5	122.0
6	99.2	115.0
7	89.9	87.5
8	85.0	79.0
9	87.5	84.0
10	102.5	125.0
11	106.5	143.0
12	92.3	91.4
13	82.5	75.0
14	93.8	97.6
15	102.1	123.5
16	99.8	115.6
17	87.9	86.6
18	81.6	74.4

Note: 1 ksi = 6.895 MPa.

The increase in steel strength at the weld seems to be the most plausible cause for the greater than expected steel shear strength results compared to those measured in air. Double shear tests of the studs conducted in the main shaft body showed good correlation with a typical reduced shear yield value.

DISCUSSION OF PROPOSED ACI CODE REQUIREMENTS

Discussed below are steel failure capacity, pryout capacity, and lightweight concrete effect.

Steel Failure Capacity

The purpose of presenting both the combined steel and weld shear failures and the stud-only shear failures introduces an important issue that must be considered in the design equations. Of the equations presented above, only the second set of equations [Eqs. (4a) and (4b)] represent the characteristic value of the connection in normal weight concrete if it is to fail due to steel shear. Eq. (4a) represents the ultimate load for a ductile steel shank failure with actual tensile strength being used, whereas Eq. (4b) uses the minimum design ultimate strength of 65 ksi (450-MPa).

For design, the equations presented above would typically be reduced by a strength reduction or phi (ϕ) factor. Arguably, the phi, or material reduction factor, should incorporate the probability that failure could occur due to a weld failure. If a value of ϕ is assumed to be 0.75, as proposed in Appendix D of the Code,[4] all tests would have failure stresses above the ultimate design stress. Additional safety factors are then built in by using a strength design criterion.

Another consideration involves the ultimate tensile strength. In this study, the value of F_{ut} ranged from 78 to 83 ksi (538 to 572 MPa) depending on stud heat and size. The current AWS standards[31] call for a minimum design tensile strength of 65 ksi (450 MPa). Ultimate tensile strengths of studs used in this study were about 20 to 25 percent greater than that used for design. Eq. (4b) is reflective of the data analysis using the minimum design ultimate strength.

Both Eqs. (4a) and (4b) above represent the calculation of a connection steel shear capacity, which is greater than the initial proposals for the new ACI 318-2002 Building Code provisions. The initial approach to steel failure was to lump embedded bolts with headed studs. The proposed ACI provisions provided the following two equations for computing the capacity of an anchorage group governed by steel failure:

A. For a fastener material with a well-defined yield point:

$$V_s = nA_{se}f_y$$

B. For cast-in fasteners without a well defined yield point:

$$V_s = n0.6A_{se}f_{ut}$$

These initial ACI proposed provisions set the capacity to the steel yield strength if the material has a well defined yield. If the embedded bolt or stud material does not have a well-defined yield point, which is the usual case, ACI defines a shear yield point of $0.6f_{ut}$.

The Appendix D design procedure involves calculating a basic connection capacity defined by the steel material. The WJE study has shown the steel capacity is governed by the-ultimate tensile strength of the fastener material, in this case a steel stud. Although the loading on these connections was almost pure shear, shear yield did not govern the steel capacity.

Under the shear yield criterion from the Energy of Distortion Theory by Huber-von Mises-Hencky, the ultimate values would be reduced to yield ($F_{vy} = 0.58F_{ut}$) or $1/\sqrt{3}$ if shear yield governed. A reduction due to shear yield, as implied by $V_s = n0.6A_{se}f_{ut}$, was not observed in the behavior and strength capacity prediction in tests reported here, and the reduction is not justified.

Pryout Capacity

The ACI Appendix D requirements for pryout appear to be somewhat cumbersome and are based only on

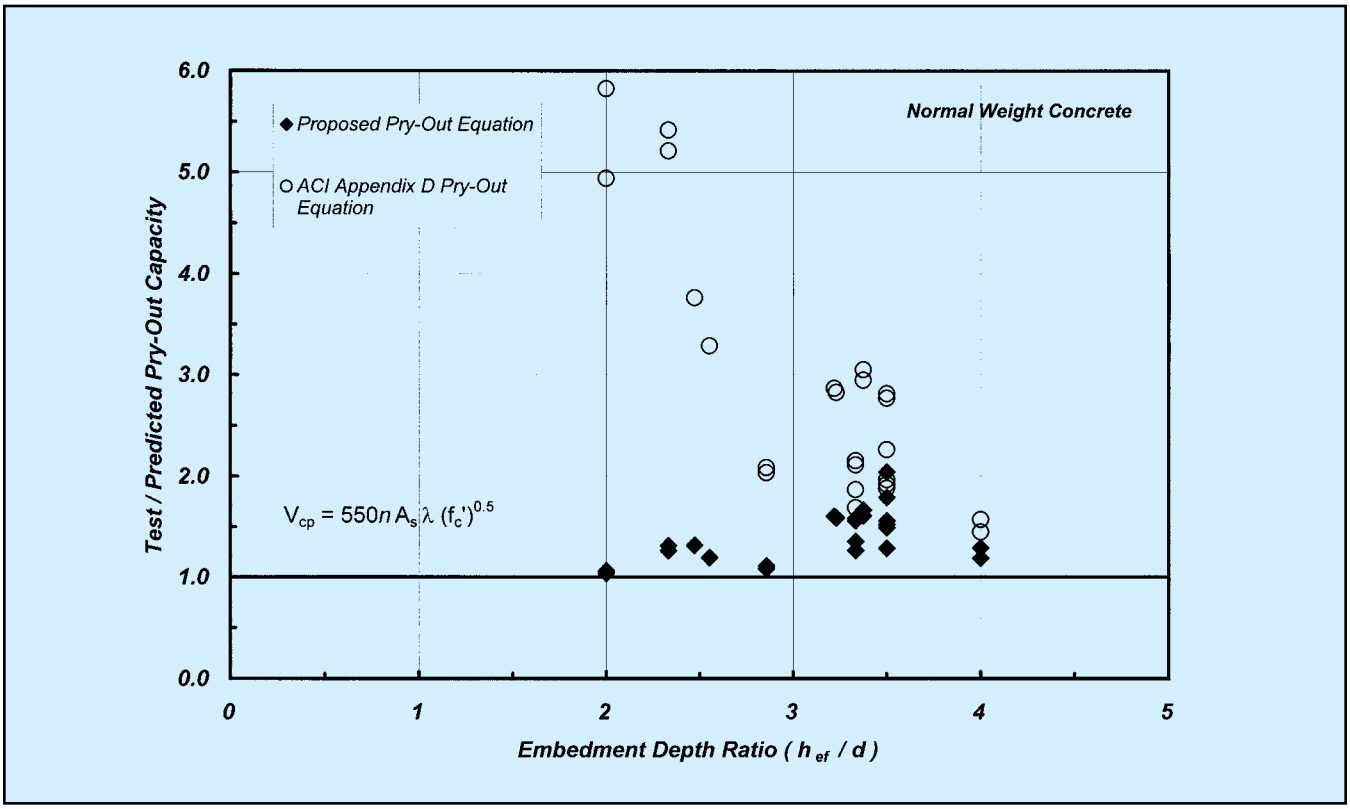

Fig. 17. Comparison of the proposed pryout equation to the ACI Appendix D proposal.

the effective embedment depth, h_{ef}. As shown in this study and in previous studies, the critical parameter for evaluating the likelihood of a concrete pryout failure for headed studs is the h_{ef}/d ratio. The critical value proposed by analysis of data in this study is 4.5, which is slightly greater than a value of 4.2 proposed by Driscoll and Slutter almost 40-years ago. Fig. 3(a) shows the WJE test data added to the earlier results for further reference.

The ACI concrete pryout capacity load requires the calculation of the tensile breakout capacity based on computing the effective area of the CCD physical model breakout surface. The provisions in ACI Appendix D[4] are as follows:

The nominal pryout strength, V_{cp}, shall not exceed:

$$V_{cp} = k_{cp} N_{cb}$$

where

k_{cp} = coefficient for pryout strength
k_{cp} = 1.0 for $h_{ef} < 2.5$ in.
k_{cp} = 2.0 for $h_{ef} > 2.5$ in.
V_{cp} = nominal concrete pryout strength (lb)
N_{cb} = nominal concrete breakout strength in tension of a single anchor (lb)

The term N_{cb} is the concrete tensile pull-out strength and is determined in accordance with the ACI 318 Appendix D requirements.

When the normal weight concrete push-off data with one *y*-row and $h_{ef}/d < 4.5$ are evaluated with the above procedure, the ACI predicted results can be overly conservative for headed studs, as depicted in Fig. 17. The inherent conservatism of the ACI equation occurs when the k_{cp} factor becomes 1.0, among other factors. Better predicted capacities were calculated with Eq. (2) for tests where pryout is a potential, as was shown in Fig. 3(b).

It must be recognized that Eq.-(2) was formulated based on data that represented some pryout results. Regardless, considering that this push-off database seems to represent the best information for short, stocky studs available at this time, the above Appendix D pryout equation is not recommended for use with headed stud anchor connections under those circumstances.

Because pryout failures will only govern in those (rare) instances when short, stocky studs are used ($h_{ef}/d <$ 4.5), a simple equation is viewed to be desirable. For computational ease, Eqs. (1) or (2) have been shown to be good prediction equations. Direct conversion of Eq. (1) yields a constant of 977 for Eq. (2), but the constant was reduced to 800 for a lower bound solution. However, neither equation represents a characteristic capacity based on a 5-percent fractile value using a 90 percent confidence level. By reviewing the push-off database for stocky stud ($h_{ef}/d < 4.5$) tests, the proposed characteristic capacity equation for headed stud pryout is:

$$V_{cp} = 550\, n\, \lambda\, A_s \sqrt{f_c'} \qquad (5)$$

where

V_{cp} = nominal shear strength (lb)
n = number of anchors in a connection group
A_s = effective cross-sectional area of a stud anchor (sq in.)
f'_c = specified compressive strength of concrete (psi)
λ = concrete unit weight factor

Predicted capacities based on proposed Eq. (5) are plotted in Fig. 17 as solid diamond shapes. Test-to-predicted ratios exceed 1.0 for the em-

bedment depth ratios (h_{ef}/d) from 2.0 to 4.0. Moreover, proposed Eq. (5) is shown as a better predictor of pryout capacity because the data points are tightly grouped with less scatter. The ACI equation, data points plotted as open circles, generally tracks above Eq. (5) predictions and has more scatter.

Lightweight Concrete Effect

Eqs. (1) and (2) have been shown to provide a good lower bound limit on stud strength in lightweight concrete, regardless of embedment depth. The steel shear failure equation in ACI 318 Appendix D does not acknowledge lightweight concrete as a variable and that a stud may not develop its full ultimate tensile strength in lightweight concrete.

When Eq. (2) is evaluated using the lightweight aggregate concrete test data from the push-off tests, Eq. (5) again is a better predictor equation for the characteristic value of capacity. The proposed Eq.-(5) is applicable for all stud embedment depths. Eq. (5) incorporates a concrete unit weight factor, λ, which accounts for the lightweight concrete effect.

Eq. (5) is thus proposed as the prediction equation for V_{cp} and V_s when a headed stud connection is embedded in lightweight concrete away from all edge influences for all embedment depths. The upper limit on V_{cp} will be $V_s = 1.0\ A_s F_{ut}$.

Further research into steel capacity in lightweight aggregate concrete may modify this capacity. Therefore, Eq. (5) is proposed to serve a two-fold capacity: determination of maximum stud capacity for anchorages located in lightweight concrete and avoidance of pryout failure in normal weight concrete for headed studs with $h_{ef}/d < 4.5$.

CONCLUSIONS AND DESIGN RECOMMENDATIONS

Given the results of the work reported herein, the following conclusions and design recommendations are presented:

Away from a Free Edge (de4)

1. For both the 1/2 and 5/8 in. (12.7 and 15.9 mm) diameter studs used in this study, steel stud failure was achieved at the minimum back edge distance of 4d. Closer back edge distances are not practical, considering clear cover requirements.

2. The WJE shear test load application produced a minimal amount of eccentricity on the connection, such that the anchorage was loaded in practically a "pure shear" condition. Small eccentricities on such an anchorage, as reported in the literature, may be sufficient enough to alter the behavior and failure mode due to the shear-tension interaction.

In-the-Field

1. When an anchorage is placed sufficiently away from all edges to negate all edge influences, termed in-the-field of the member, the connection will achieve a capacity based on all headed studs failing in a steel failure mode. Assuming the weld quality is adequate, the failure will be ductile with appreciable lateral deformation.

2. For the two- and four-stud anchorages tested in this program, the x- and y-spacings of 4.5d and 7.0d in different combinations and load application direction had no influence on the failure mode, that is, steel stud shear, and did not have a significant effect on the ultimate capacity of the anchorage. From a review of the literature, the proposed ACI minimum x-spacing in an anchorage of 4d seems appropriate.

3. Although the WJE tests did not exhibit a reduction in anchorage capacity, large y-spacings of the studs, as reported in the literature, can produce a shear lag effect. Shear lag reduces the efficiency of the connection failing in a stud steel mode.

Capacity Based on Steel Failure

1. For anchorages governed by steel stud shank failure, this study shows the ultimate shear failure load is best predicted using the ultimate tensile strength of the stud. Eq. (4b) is recommended as the steel prediction equation (V_s) for headed studs in normal weight concrete with $h_{ef}/d > 4.5$.

2. Steel stud failures in this study were achieved with well-embedded studs. It is proposed that a well-embedded stud have a minimum effective embedment-to-diameter ratio (h_{ef}/d) of 4.5, as determined by reviewing tests in the literature. The minimum h_{ef}/d ratio of studs used in this study was 5.30.

3. Headed studs with an h_{ef}/d less than 4.5 will precipitate a failure mode known as pryout. This failure mode produces an ultimate capacity less than that predicted by $1.0\ A_s F_{ut(design)}$. Eq. (5) is proposed to predict the capacity for short, "stocky" studs having $h_{ef}/d < 4.5$.

4. A review of limited test data on stud anchorage failures in lightweight concrete shows that the stud cannot develop its full capacity based on $1.0\ A_s F_{ut}$. From the information available at this time, a maximum stud capacity based on Eq.-(5) is proposed. Eq. (5), which is a concrete predictor equation, is appropriate because the ultimate connection capacity in lightweight concrete is dependent on a combination of local concrete crushing and increased stud deformation.

5. The minimum connection plate thickness of one-half the stud diameter (0.5d) presently in the PCI Handbook is slightly conservative for a "pure shear" loaded connection. The practical minimum to achieve steel stud failure was experimentally determined to be 0.37d or (3/8)d, as reported in the literature. Increased plate thickness may be required for bending resistance or to ensure a more uniform load distribution to the attached studs. The plate thickness used in this study was 1/2 in. (12.7 mm), thus exceeding the minimum suggested limits.

Based on the results of this study summarized above, concise design recommendations for the shear capacity of an anchorage failing in a steel stud failure mode are conveniently presented in the flowchart of Fig. 18.

Research Needs

Additional work is needed in determining the ultimate capacity of a connection located in-the-field of a lightweight concrete member. To date, most work on cast-in headed stud anchorages has been performed in nor-

mal weight concrete. Lightweight concrete is used by the precast concrete industry in numerous applications, many of which use connections with large distances from member edges.

Connections with a large *y*-spacing of studs, or an overall large out-to-out *y*-spacing, located in-the-field of a member need further study with respect to shear-lag effects. A determination of the maximum individual or overall *y*-spacing permissible to preclude shear lag reduction would seem appropriate. Moreover, an efficiency factor for connections affected by shear lag may be required. Guidance for this influence can be found in research for load transfer mechanisms in long, high strength bolted connections.

ACKNOWLEDGMENTS

Wiss, Janney, Elstner Associates, Inc. wishes to express its appreciation to the Precast/Prestressed Concrete Institute for sponsoring this research project. In particular, the authors wish to thank PCI's Research and Development Committee and the members of the Industry Advisory Group (Thomas J. D'Arcy, chairman) for their constructive comments during the course of this project.

Gratitude is expressed to Harry Chambers and Nelson Stud Welding, Elyria, Ohio for their contributions of technical training, stud material donation, stud welder use, and additional laboratory support in Ohio. Thanks are also expressed to Thomas Soukup and Michael Pistilli of Prairie Materials, Bridgeview, Illinois for their gracious donation of the (consistent) concrete material for the project, Kevin Heinert of Williams Form Engineering for the high-strength coil rod used as part of the loading framework, and Roy Edgar of Dayton-Richmond for supplying slab lifting hardware.

Publications cited in the literature were oftentimes difficult to locate, especially the push-off literature and reports from the 1960s. Special thanks is extended to Dr. James Baldwin, Civil Engineering Professor Emeritus, University of Missouri-Columbia for locating and loaning WJE numerous out-of-print University of Missouri research reports and engineering experimental station bulletins.

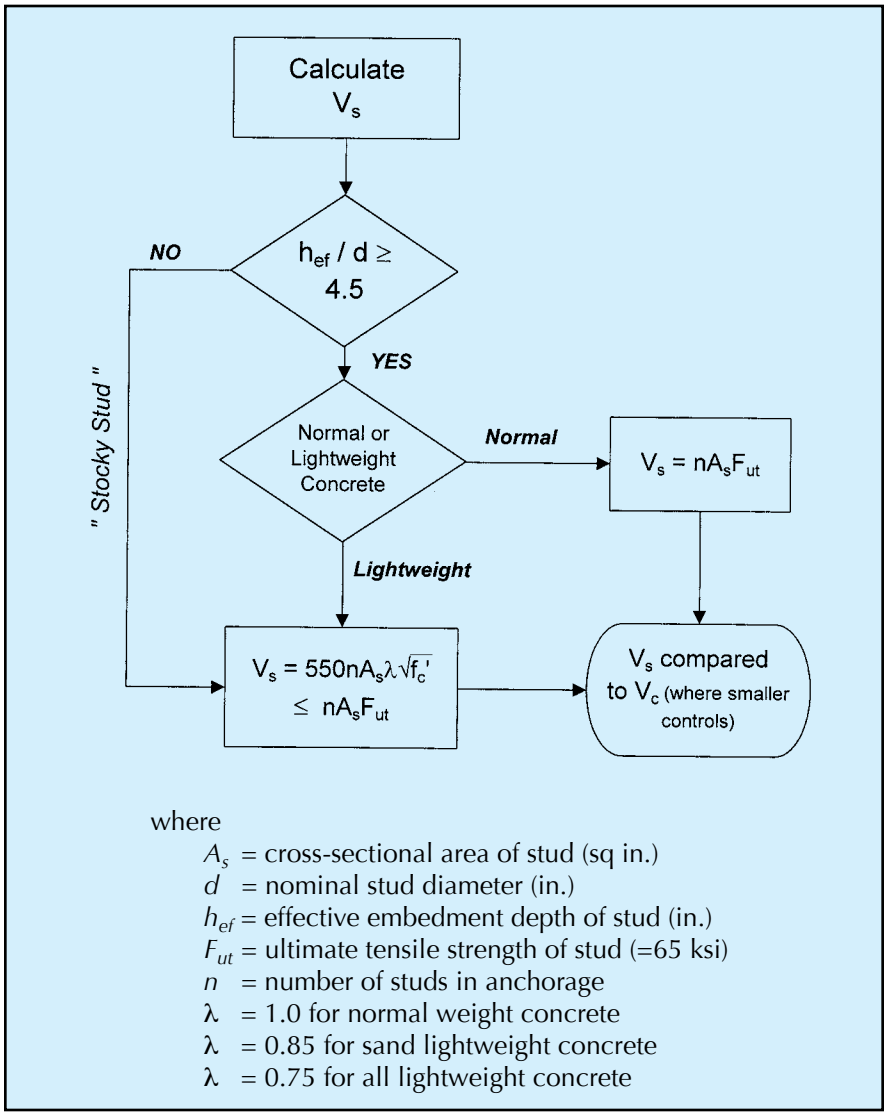

Fig. 18. Flowchart showing recommended maximum capacity of a headed stud anchorage.

REFERENCES

1. *PCI Design Handbook*, Fifth Edition (PCI MNL 120-99), Precast/Prestressed Concrete Institute, Chicago, IL, 1999.
2. ACI Committee 349, "Code Requirements for Nuclear Safety Related Concrete Structures (ACI 349-97)," *ACI Manual of Concrete Practice*, Part 4, American Concrete Institute, Farmington Hills, MI, 2000.

3. ACI Committee 318, "Building Code Requirements for Structural Concrete (ACI 318-99) and Commentary (ACI 318R-99)," American Concrete Institute, Farmington Hills, MI, 1999.
4. ACI Committee 318-B, Appendix D - Anchoring to Concrete, Code CB-30, June 22, 2000, Draft Version, American Concrete Institute, Farmington Hills, MI, 17 pp.
5. Fuchs, W., Eligenhausen, R., and Breen, J. E., "Concrete Capacity Design (CCD) Approach for Fastening to Concrete," *ACI Structural Journal*, V. 92, No. 1, January-February 1995, pp. 73-94.
6. Anderson, N. S., and Meinheit, D. F., "Design Criteria for Headed Stud Groups in Shear," PCI Research Report, Precast/Prestressed Concrete Institute, Chicago, IL, under preparation.
7. Viest, I. M., "Investigation of Stud Shear Connectors for Composite Concrete and Steel T-Beams," *Journal of the American Concrete Institute*, V. 27, No. 8, April 1956, pp. 875-891.
8. Driscoll, G. C., and Slutter, R. G., "Research on Composite Design at Lehigh University," Proceedings, AISC National Engineering Conference (May 11-12, 1961), Minneapolis, MN, 1961, pp. 18-24.
9. Ollgaard, J. G., Slutter, R. G., and Fisher, J. W., "Shear Strength of Stud Connectors in Lightweight and Normal-Weight Concrete," *AISC Engineering Journal*, V. 8, No. 2, April 1971, pp. 55-64.
10. Baldwin, Jr., J. W., "Composite Bridge Stringers – Final Report," Report 69-4, Missouri Cooperative Highway Research Program, Missouri State Highway Department and University of Missouri-Columbia, MO, May 1970, 62 pp.
11. Buttry, K. E., "Behavior of Stud Shear Connectors in Lightweight and Normal-Weight Concrete," Report 68-6, Missouri Cooperative Highway Research Program, Missouri State Highway Department and University of Missouri-Columbia, MO, August 1965, 45 pp.
12. Dallam, L. N., "Push-Out Tests of Stud and Channel Shear Connectors in Normal-Weight and Lightweight Concrete Slabs," Bulletin Series No. 66, Engineering Experiment Station, University of Missouri-Columbia, Columbia, MO, April 1968, 76 pp.
13. Goble, G. G., "Shear Strength of Thin Flange Composite Specimens," *AISC Engineering Journal*, V. 5, No. 2, April 1968, pp. 62-65.
14. Chinn, J., "Pushout Tests on Lightweight Composite Slabs," *AISC Engineering Journal*, V. 2, No. 4, October 1965, pp. 129-134.
15. Hawkins, N. M., "The Strength of Stud Shear Connectors," Research Report No. R141, Department of Civil Engineering, University of Sydney, Sydney, Australia, December 1971, 34 pp.
16. Kulak, G. L., Fisher, J. W., and Struik, J. H. A., *Guide to Design Criteria for Bolted and Riveted Joints*, Second Edition, John Wiley and Sons, New York, NY, 1987, 333 pp.
17. Viest, I. M., "Studies of Composite Construction at Illinois and Lehigh, 1940-1978," *Composite Construction in Steel and Concrete III*, Proceedings of an Engineering Foundation Conference, Irsee, Germany (June 9-14, 1996), Edited by C. D. Buckner and B. M. Shahrooz, American Society of Civil Engineers, New York, NY, 1997, pp. 1-14.
18. Seely, F. B., and Smith, J. O., *Advanced Mechanics of Materials*, Second Edition, John Wiley & Sons, Inc., New York, NY, 1952, pp.76-91.
19. AASHO, *Standard Specifications for Highway Bridges*, Eighth Edition, American Association of State Highway Officials, Washington, DC 1961.
20. AISC, *Manual of Steel Construction*, Eighth Edition, American Institute of Steel Construction, Chicago, IL, 1980.
21. Shaikh, A. F., and Yi, W., "In Place Strength of Welded Headed Studs," PCI JOURNAL, V. 30, No. 2, March-April 1985, pp. 56-81.
22. *PCI Design Handbook*, Fourth Edition (PCI MNL 120-92), Precast/Prestressed Concrete Institute, Chicago, IL, 1992.
23. *PCI Design Handbook*, First Edition, Prestressed Concrete Institute, Chicago, IL, 1971.
24. *PCI Design Handbook*, Second Edition, Prestressed Concrete Institute, Chicago, IL, 1978.
25. *PCI Design Handbook*, Third Edition, Prestressed Concrete Institute, Chicago, IL, 1985.
26. AISC, *Manual of Steel Construction – Load & Resistance Factor Design (LRFD)*, Volume I (Structural Members, Specifications & Codes), Second Edition, American Institute of Steel Construction, Chicago, IL, 1994.
27. CISC, *Handbook of Steel Construction*, Fifth Edition, Canadian Institute of Steel Construction, Willowdale, Ontario, Canada, 1991.
28. AASHO, *Standard Specifications for Highway Bridges*, Ninth Edition, American Association of State Highway Officials, Washington, DC, 1965.
29. AWS, *Supplement to AWS D1.0-66, Code for Welding in Building Construction and AWS D2.0-66, Specifications for Welded Highway and Railway Bridges on Requirements for Stud Welding*, September 1968, American Welding Society, Inc., New York, NY, 12 pp.
30. AWS, *Structural Welding Code*, AWS D1.1-82, Sixth Edition, American Welding Society, Miami, FL, 1982.
31. AWS, *Structural Welding Code – Steel, AWS D1.1:2000*, 17th Edition, American Welding Society, Miami, FL, 2000.
32. ASTM, *Standard Specification for Steel Bars, Carbon, Cold-Finished, Standard Quality* (ASTM A108-99), Volume 04.07, American Society for Testing and Materials, West Conshohocken, PA, 1999.
33. Kuhn, D. P., and Shaikh, A. F., "Pilot Study on Headed Anchor Studs: A Comparison Between PCI and CCD," Interim Report, Department of Civil Engineering, University of Wisconsin, Milwaukee, WI, August 1997, 29 pp.
34. Wollmershauser, R. E., "Anchor Performance and the 5% Fractile," *Hilti Technical Services Bulletin*, November 1997, Hilti, Inc., Tulsa, OK, 5 pp.
35. Linnert, G. E., *Welding Metallurgy – Carbon and Alloy Steels, Volume I – Fundamentals*, Fourth Edition, American Welding Society, Miami, FL, 1994.
36. Nelson Stud Welding, "Hardness Profile Testing of Wiss, Janney, Elstner/Precast Concrete Institute Shear Test Specimen," Test Report No. 2000-2, Nelson Stud Welding, Elyria, OH, 2000, 5 pp.
37. ASTM, *Standard Hardness Conversion Tables for Metals (Relationship Among Brinell Hardness, Vickers Hardness, Rockwell Hardness, Rockwell Superficial Hardness, Knoop Hardness, and Scleroscope Hardness)* (ASTM E140-97e2), Volume 03.01, American Society for Testing and Materials, West Conshohocken, PA, 1999.

APPENDIX — NOTATION

A_s = effective cross-sectional area of stud anchor (sq in.)
A_{se} = effective cross-sectional area of stud anchor (sq in.) (Appendix D notation)
d = shaft diameter of headed stud (in.)
de1 = side edge distance normal to shear load application direction, parallel to *x*-axis, taken from center of anchor shaft to the side concrete edge (in.) (see Fig. 1)
de2 = side edge distance normal to shear load application direction, parallel to *x*-axis, taken from center of anchor shaft to side concrete edge (in.) (see Fig. 1, de2 is the side edge distance opposite de1)
de3 = front edge distance parallel to shear load application direction and *y*-axis taken from center of front anchor shaft to front concrete edge (in.) (see Fig. 1)
de4 = back or rear edge distance parallel to shear load application direction and *y*-axis, taken from center of back anchor shaft to rear concrete edge (in.) (see Fig. 1)
E_c = modulus of elasticity of concrete (psi)
f'_c = specified compressive strength of concrete (psi)
$F_{ut(actual)}$ = actual ultimate tensile strength of headed stud steel in tension (psi)
$F_{ut(design)}$ = design minimum tensile strength of anchor steel in tension (psi) (see Table 3)
F_{ut}, f_{ut} = specified ultimate tensile strength of anchor steel in tension (psi)
F_{vy} = shear yield strength of anchor steel (psi)
F_y, f_y = specified yield strength of anchor steel in tension (psi)
h = thickness of concrete member in which anchors are embedded, measured parallel to anchor axis (in.) (see Fig. 1)
h_{ef} = effective headed stud embeddment depth taken as length under head to concrete surface (in.) (see Fig. 1)
k_{cp} = coefficient for pryout stength (from ACI Appendix D)
L = overall length in the *y*-direction between outermost anchors in conncetion = $\sum y$ (in.) (from AISC)
n = number of anchors in connection or group
N_{cb} = nominal concrete breakout strength in tension of single anchor (lb) (from ACI Appendix D)
Q = nominal stength of stud shear connector embedded in solid concrete slab (lb) (from AISC)
t = thickness of attachment plate (in.)
t_f = flange thickness of a structural steel shape (in.)
V_{cp} = nominal concrete pryout stength (lb) (from ACI Appendix D
V_n = nominal shear strength (lb)
V_s, V_{steel} = nominal shear stength of single headed stud or group of headed studs governed by steel strength
x = center-to-center spacing of stud anchors in *x* direction of Cartesian plane (in.) (see Fig. 1)
$\bar{x}$ = eccentricity between shear plane and centroidal axis of connected component (in.) (from AISC)
y = center-to-center spacing of stud anchors in the *y* direction of Cartesian plane (in.) (see Fig. 1)
λ = concrete unit weight factor
= 1.0 for normal weight concrete
= 0.85 for sand lightweight concrete
= 0.75 for all lightweight concrete
κ = one-sided population limit (fractile) factor for a normal distribution
μ = coefficient of friction
ϕ = strength reduction factor